

# **Investigation of molecular weight effects during the solution crystallisation of polyolefins**

**M Brand**

Thesis presented in partial fulfilment of the requirements for the degree of  
Master of Science at the University of Stellenbosch.



Study Leader: Dr A.J van Reenen.

March 2008

## **Declaration**

By submitting this thesis electronically, I declare that the entirety of the work contained therein is my own, original work, that I am the owner of the copyright thereof (unless to the extent explicitly otherwise stated) and that I have not previously in its entirety or in part submitted it for obtaining any qualification.

Date: March 2008.

## Abstract

This study involved (a) the development and testing of a solution turbidity fractionation analyser (TFA) and (b) the investigation of possible molecular weight effects on solution crystallisation. To investigate the latter highly isotactic polypropylene was polymerised with a C<sub>2</sub> symmetric metallocene catalyst. Blends were made of these homopolymers. The homopolymers as well as the blends were fractionated by means of temperature rising elution fractionation (TREF). The fractionated and unfractionated homopolymers as well as the fractionated blends were characterised by <sup>13</sup>C NMR, differential scanning calorimetry (DSC) and gel permeation chromatography (GPC). The TFA was successfully developed and helped in explaining the shifting of solution crystallisation temperature that was seen when blending of the homopolymers occurred. This was done performing analyses on the machine of blends of the homopolymers. Fractions, of the homopolymers and blends, obtained from TREF were also done. Subsequent runs of blends made from the fractions obtained from TREF were also done. In the end it was shown that the shift of the solution crystallisation temperature is either due to the tacticity or the molecular weight depending on the sample.

## Opsomming

Hierdie navorsing het die volgende behels: (a) die ontwikkeling en evaluering van 'n oplossing turbiditeit fraksionering analiseerder (TFA) en (b) ondersoek na moontlike molekulêre massa effekte gedurende kristallisatie uit oplossing. Hoogs isotaktiese polipropileen is gesintetiseer met 'n  $C_2$  simmetriese katalis om die laasgenoemde te ondersoek. Mengsels van hierdie homopolimere is gemaak. Beide die homopolimere en die mengsels is gefraksioneer deur middel van temperatuurstyging eluering fraksionering (TREF). Karakterisering van die gefraksioneerde en ongefraksioneerde homopolimere sowel as die gefraksioneerde mengsels is deur middel van  $^{13}C$ -KMR, differensiële skandeer kalorimetrie (DSC) en jel-permeasie kromatografie (GPC) gedoen. Die ontwikkeling van die TFA was suksesvol en het bygedra om die verskuiwing in kristallisatie temperatuur in oplossing, wat waargeneem is wanneer die homopolimere gemeng is, te kon verduidelik. Bostaande is vermag deur analyses van die mengsels van die homopolimere te doen sowel as die fraksies van die homopolimere en mengsels wat van TREF verkry is. Mengsels van fraksies wat vanaf TREF verkry is is ook deur die TFA geanaliseer. Daar is sodoende bewys dat of taktisiteit of die molekulêre massa, afhangende van die monster, die verskuiwing van die kristallisatie temperatuur in oplossing veroorsaak.

This thesis is dedicated to my Mother  
-Thanks Mom-

## Acknowledgements

I wish to express my sincere gratitude and thanks to the following people:

**Dr. AJ van Reenen** for his guidance and support throughout this study and for believing in me even before I was his student

**Gareth Harding** for the GPC work

**Jean McKenzie** and **Elsa Malherbe** for the  $^{13}\text{C}$ -NMR analysis

**Prof Walters** and **Johan Germishuizen** for all the assistance during the development of the TFA

The **Olefins** research group

**Erinda, Aneli, Margie** and **Calvin** for administrative and technical assistance

**Elana** and **Phillip**, without their persistence and unwavering support I would not even be here and I am especially grateful for all the lighter moments throughout the studies

**Gareth B, Liesl, Morné, Adine, Francois, Jerrie, Rassie, Gunter** and **Gareth H** for being there to listen, give moral support, making me laugh and reminding me it is not as bad as it seems

To my family; my **Mom, Liezl** and **Willem** for endless support and encouragement

To **SASOL** and **NRF** for funding

# Table of Contents

List of Equations .....	V
List of Figures.....	VI
List of Schemes.....	IX
List of Tables .....	X
Abbreviations .....	XI
<b>Chapter 1.....</b>	<b>1</b>
<i>Introduction and Objectives.....</i>	<i>1</i>
General Introduction .....	2
1.1 Aims.....	2
1.2 Objectives .....	2
1.3 References .....	4
<b>Chapter 2.....</b>	<b>5</b>
<i>Historical Background and Literature review.....</i>	<i>5</i>
2.1 Polypropylene.....	6
2.2 Metallocene catalysed polymers.....	7
2.3 Molecular weight control in metallocenes .....	11
2.3.1 Influence of addition of hydrogen to control molecular weight.....	11
2.3.2 Molecular weight control by means of structural effects .....	11
2.4 Crystallisation of isotactic polypropylene .....	12

<b>2.5</b>	<b>Molecular weight effects on crystallisation .....</b>	<b>13</b>
<b>2.6</b>	<b>Fractionation Techniques for Semi-crystalline polymers .....</b>	<b>15</b>
2.6.1	Temperature Rising Elution Fractionation .....	16
2.6.2	Turbidity analysis .....	18
<b>2.7</b>	<b>Summary .....</b>	<b>19</b>
<b>2.8</b>	<b>References .....</b>	<b>20</b>

## **Chapter 3..... 22**

### ***Experimental* 22**

<b>3.1</b>	<b>Polymerisation.....</b>	<b>23</b>
3.1.1	Materials .....	23
3.1.2	Preparation of the catalyst .....	23
3.1.3	Homogeneous polymerisation of polypropylene .....	23
<b>3.2</b>	<b>Characterisation .....</b>	<b>24</b>
3.2.1	High temperature gel permeation chromatography (HT-GPC) .....	24
3.2.2	Nuclear magnetic resonance (NMR) .....	24
3.2.3	Differential scanning calorimetry (DSC).....	25
3.2.4	Temperature rising elution fractionation analysis (TREF).....	25
3.2.5	Turbidity fractionation analyser .....	26
<b>3.3</b>	<b>References .....</b>	<b>28</b>



**Chapter 4 ..... 29**

***Development of a Turbidity fractionation analyser ..... 29***

**4.1 Introduction..... 30**

**4.2 Turbidity analyser..... 30**

**4.3 Chemically distinct polymers..... 32**

**4.4 Effect of experimental parameters..... 34**

4.4.1 Sample concentration effects ..... 34

4.4.2 Cooling rate ..... 35

4.4.3 Heating rate ..... 36

4.4.4 Molecular weight effects ..... 37

**4.5 References ..... 39**

**Chapter 5..... 40**

***Results and Discussion ..... 40***

**5.1 Characterisation of the metallocene  
isotactic polypropylene homopolymers..... 41**

5.1.1 The unfractionated metallocene homopolymers..... 41

5.1.2 The fractionated metallocene homopolymers..... 44

**5.2 Turbidity Data ..... 54**

**5.3 Summary ..... 63**

**5.4 References ..... 64**

**Chapter 6..... 65**

***Conclusion and Recommendations ..... 65***

6.1 Conclusions .....66

6.2 Recommendations .....67

Appendix A .....68

Appendix B .....79

# List of Equations

<b>Equation 2.1:</b> The Avrami equation for films .....	13
<b>Equation 2.2:</b> The Avrami equation for bulk samples .....	13
<b>Equation 2.3:</b> The Flory-Huggins equation for free energy of mixing.....	16

# List of Figures

<b>Figure 2.1:</b> Generic structure of a metallocene catalyst where Mt is the metal (Ti, Zr, Hf), E is the bridging group (R <sub>2</sub> C, R <sub>2</sub> Si, -CH <sub>2</sub> -CH <sub>2</sub> -), X is 2 e <sup>-</sup> σ-ligand (Cl, Me) and L is a η <sup>5</sup> ligand.....	7
<b>Figure 3.2:</b> Experimental setup of the turbidity fractionation analyzer.....	26
<b>Figure 4.3:</b> Schematic diagram of the turbidity fractionation analyser, as viewed from the top.....	31
<b>Figure 4.4:</b> Raw data, cooling scan of M-iPP-3, 2 °C /minute, concentration of 2 mg/mL.....	33
<b>Figure 4.5:</b> First derivative of raw data shown in Figure 4.4.....	33
<b>Figure 4.6:</b> Comparison of a propylene-1-pentene copolymer and LLDPE analyzed under identical conditions (2 mg/mL, 2 °C/min).....	34
<b>Figure 4.7:</b> Concentration effects during crystallisation from solution for a propylene-1-1-pentene copolymer.....	35
<b>Figure 4.8:</b> The effect of cooling rate on the crystallisation of PP-1 Pentene. Cooling rates of 1, 1.4 and 2 °C were used. The solution concentration was 1 mg/mL.....	36
<b>Figure 4.9:</b> The heating profiles of 1 mg/mL solutions of a PP-1-pentene copolymer. Heating rates of 1 and 2 °C/minute are shown. ....	37
<b>Figure 4.10:</b> Crystallisation profiles of two polypropylenes prepared by a metallocene catalyst. The dashed line represents the polymer with a molecular weight of 134 984, while the solid line represents a polymer with a molecular weight of 35 962. Sample concentration was 2 mg/mL and cooling rate 2 °C/min.....	38
<b>Figure 5.11:</b> NMR spectrum of M-iPP1 with insert of isotactic peaks.....	41
<b>Figure 5.12:</b> <sup>13</sup> C NMR spectrum showing 2,1 and 3, 1 insertions as well as different endgroups of M-iPP-5.....	43
<b>Figure 5.13:</b> <sup>13</sup> C NMR showing the 2,1 insertions in M-iPP-4 .....	43
<b>Figure 5.14:</b> TREF overlay of the homopolymers.....	45
<b>Figure 5.15:</b> TREF overlay of the blends.....	47
<b>Figure 5.16:</b> Weighted Fraction versus elution temperature for M-iPP 1+4 .....	51
<b>Figure 5.17:</b> Mw versus elution temperature for the M-iPP 1+4 blend and homopolymers .....	52
<b>Figure 5.18:</b> Weighted Fraction versus elution temperature for M-iPP 3 + 4 .....	53

<b>Figure 5.19:</b> Weighted Fraction versus elution temperature for M-iPP 5 + 6 .....	53
<b>Figure 5.20:</b> Typical Response of a cooling experiment with the turbidity analyser .....	54
<b>Figure 5.21:</b> First derivative of the turbidity data .....	55
<b>Figure 5.22:</b> Overlay of the original homopolymers, similar tacticity different Mw, and the corresponding blend from the TFA data .....	55
<b>Figure 5.23:</b> Overlay of the same Mw differing tacticity.....	56
<b>Figure 5.24:</b> TFA of two samples with differing Mw and tacticity.....	57
<b>Figure 5.25:</b> TFA experiment on the 100°C fractions for M-iPP-1, M-iPP-4 and M-iPP-1+4.....	58
<b>Figure 5.26:</b> TFA experiment on the 110°C fractions of the homopolymers and blend.....	58
<b>Figure 5.27:</b> TFA cooling experiment on the 100 °C fractions of M-iPP-3, M-iPP- 4 and M-iPP-3+4.....	59
<b>Figure 5.28:</b> TFA cooling experiment on the 110°C fraction of M-iPP-3, M-iPP-4 and M-iPP3+4.....	60
<b>Figure 5.29:</b> TFA experiment on the 110 °C fraction of the M-iPP-3 and M-iPP-4 polymer as well as the subsequent blend.....	61
<b>Figure 5.30:</b> TFA experiments of the 100°C fraction of M-iPP-5, M-iPP-6 and M- iPP5+6 .....	62
<b>Figure 5.31:</b> TFA experiment of the 110°C fraction of the M-iPP-5, M-iPP-6 and M-iPP-5+6 polymers .....	62
<b>Figure 5.32:</b> TFA experiment of the 110°C fraction of the homopolymers and a blend of it .....	63
<b>Figure A.33:</b> NMR spectrum of the unfractionated M-iPP-1 homopolymer .....	68
<b>Figure A.34:</b> NMR spectrum of the unfractionated M-iPP-2 homopolymer. ....	68
<b>Figure A.35:</b> NMR spectrum of the unfractionated M-iPP-3 homopolymer .....	69
<b>Figure A.36:</b> NMR spectrum of the unfractionated M-iPP-4 homopolymer. ....	69
<b>Figure A.37:</b> NMR spectrum of the unfractionated M-iPP-5 homopolymer. ....	70
<b>Figure A.38:</b> NMR spectrum of the unfractionated M-iPP-6 homopolymer. ....	70
<b>Figure A.39:</b> NMR spectrum of the 100°C fraction of the M-iPP-2+3 blend.....	71
<b>Figure A.40:</b> NMR spectrum of the 110°C fraction of the M-iPP-2+3 blend.....	71
<b>Figure A.41:</b> NMR spectrum of the 100°C fraction of the M-iPP-3+4 blend .....	72
<b>Figure A.42:</b> NMR spectrum of the 110°C fraction of the M-iPP-3+4 blend.....	72
<b>Figure A.43:</b> NMR spectrum of the 90°C fraction of the M-iPP-5+6 blend .....	73
<b>Figure A.44:</b> NMR spectrum of the 100°C fraction of the M-iPP-5+6 blend.....	73

<b>Figure A.45:</b> NMR spectrum of the 110°C fraction of the M-iPP-5+6 blend .....	74
<b>Figure A.46:</b> NMR spectrun of the 100°C fraction of M-iPP-1 homopolymer .....	74
<b>Figure A.47:</b> NMR spectrum of the 110°C fraction of M-iPP-1 homopolymer .....	75
<b>Figure A.48:</b> NMR spectrum of the 100°C fraction of M-iPP-4 homopolymer .....	75
<b>Figure A.49:</b> NMR spectrum of the 110°C fraction of M-iPP-4 .....	76
<b>Figure A.50:</b> NMR spectrum of the 100°C fraction of M-iPP-5 .....	76
<b>Figure A.51:</b> NMR spectrum of the 110°C fraction of M-iPP-5 .....	77
<b>Figure A.52:</b> NMR spectrum of the 100°C fraction of M-iPP-6 .....	77
<b>Figure A.53:</b> NMR spectrum of the 110°C fraction of M-iPP-6 .....	78
<b>Figure B.54:</b> DSC thermogram overlay of the homopolymers .....	79
<b>Figure B.55:</b> DSC thermogram overlay of the fractions obtained from TREF for homopolymer M-iPP-1 .....	79
<b>Figure B.56:</b> DSC thermogram overlay of the fractions obtained from TREF for the homopolymer of M-iPP-3 .....	80
<b>Figure B.57:</b> DSC thermogram overlay of the fractions obtained from TREF for the homopolymer of M-iPP-5 .....	80
<b>Figure B.58:</b> DSC thermogram overlay of the fractions obtained from TREF for the homopolymer M-iPP-6 .....	81
<b>Figure B.59:</b> DSC thermogram overlay of the fractions obtained from TREF for the blend of M-iPP-1+4 .....	81
<b>Figure B.60:</b> DSC thermogram overlay of the fractions obtained from TREF for the blend of M-iPP2+3 .....	82
<b>Figure B.61:</b> DSC thermogram overlay of the fractions obtained from TREF for the blend of M-iPP-3+4 .....	82
<b>Figure B.9:</b> DSC thermogram overlay of the fractions obtained from TREF for the blend of M-iPP-5+6	

# List of Schemes

<b>Scheme 2.1:</b> The three major types of polypropylene tacticities .....	6
<b>Scheme 2.2:</b> The role of MAO in the activation and polymerisation of a metallocene catalyst. ....	8
<b>Scheme 2.3:</b> Microstructure obtained depending on the stereocontrol mechanism .....	9
<b>Scheme 2.4:</b> Primary insertion of propylene into the metal carbon bond .....	10
<b>Scheme 2.5</b> Types of errors that can occur during polymerisation of metallocene i-PP .....	10
<b>Scheme 2.6:</b> The mechanism of direct insertion of H <sub>2</sub> into the metal-carbon bond.....	11
<b>Scheme 2.7:</b> β-Hydrogen transfer to the monomer in C <sub>2</sub> -symmetric metallocene polymerisation leading to chain termination.....	12
<b>Scheme 2.8:</b> Illustration of the two steps during a TREF experiment.....	17

# List of Tables

<b>Table 2.1:</b> Summary of the number average molecular ( $\overline{M}_n$ ) weight of the two main fractions of iPP-56, iPP-57 and iPP-68.....	14
<b>Table 2.2:</b> Comparison of analytical TREF and p-TREF .....	18
<b>Table 4.3:</b> Characterisation data for the polyolefins used in this study.....	32
<b>Table 5.4:</b> Summary of $M_w$ , $M_n$ , melting temperature and crystallinity of metallocene i-PP.....	42
<b>Table 5.5:</b> Summary of the DSC data for the homopolymers .....	42
<b>Table 5.6:</b> Summary of the GPC data of the fractionated homopolymers .....	46
<b>Table 5.7:</b> Isotacticity of the individual samples obtained by TREF.....	48
<b>Table 5.8:</b> Isotacticity of the TREF fractions of the blends .....	49
<b>Table 5.9:</b> GPC and DSC data of the fractionated blends.....	50



# Abbreviations

CRYSTAF	Crystallisation analysis fractionation
DSC	Differential scanning calorimetry
$T_m$	Equilibrium melting temperature of the polymer in solution
$\chi_1$	Flory-Huggins thermodynamic interaction parameter
GPC	Gel permeation chromatography
$\Delta H_u$	Heat of fusion per repeating unit
i-PP	Isotactic polypropylene
$T_m$	Melting temperature of the polymer
M-iPP	Metallocene isotactic polypropylene
MAO	Methylaluminoxane
$V_u$ and $V_1$	Molar volumes of the polymer repeating unit and diluent respectively
NMR	Nuclear magnetic resonance
$\overline{M}_n$	Number average molecular weight
x	Number of segments
PP	Polypropylene
PDI	Polydispersity index
p-TREF	Preparative temperature rising elution fractionation
MBI	<i>rac</i> -Me <sub>2</sub> Si(2-Me-Benz[e]ind) <sub>2</sub> ZrCl <sub>2</sub>
SCBD	Short chain branching distribution
$T_c$	Crystallisation temperature
TREF	Temperature rising elution fractionation
TFA	Turbidity fractionation analyzer
$v_1$ and $v_2$	Volume fractions of the diluent and polymer respectively
$\overline{M}_w$	Weight average molecular weight

# Chapter 1

## Introduction and Objectives

*This chapter gives a brief introduction to metallocene polymerisation and subsequent techniques used to characterise and analyse semi-crystalline polymers.*

## 1.1 General Introduction

Polyolefins are widely used and the market demand keeps growing yearly<sup>1</sup>. Polypropylene is a versatile polymer that due to the prochiral nature of the monomer can form different structures from atactic polypropylene to isotactic polypropylene. Commercially, Ziegler-Natta catalysts are used to polymerise polypropylene but metallocene catalysts give more freedom in producing polypropylene with tailor-made structures. The importance of fast screening techniques to characterise polymers is very important. Techniques such as gel permeation chromatography to obtain molecular weight data, differential scanning calorimetry for melting point, crystallisation temperature and crystallinity (%) are very useful. Other more recent techniques such as temperature rising elution chromatography (TREF) and crystallisation analysis fractionation (CRYSTAF) can give plenty of data including short chain branching distribution. With preparative TREF (p-TREF) the collected fractions can be characterised further by other techniques.

Within the field of study of the crystalliation behaviour of polyolefins certain assumptions have always been made with regard to the effect of molecular weight on the crystallisation process. In some previous studies in this group, we have noticed an apparent molecular weight effect during the use of p-TREF<sup>2,3</sup>. In this study we set out to test the assumption that molecular weight does in fact have a role in the solution crystallisation of isotactic polyolefins. At the same time, we were developing a new analytical instrument for checking the solution crystallisation of the polyolefins, based on an instrument reported by Shan et al<sup>4</sup>.

## 1.2 Aims

The overall aims of the project were to (a) test the effect of molecular weight on fractionation by crystallisation procedures, and (b) to develop and test a turbidity fractionation analyser. The objectives set out to achieve the aims are set out below.

## 1.3 Objectives

The main objectives of this research study were as follow.

- Polymerising of highly isotactic polypropylene with differing molecular weight.
- Characterisation of the homopolymers that were synthesized by NMR, GPC and DSC.
- Fractionation of the homopolymers with subsequent characterisation of the fractions.
- Blending of homopolymers and subsequently fractionating the blends.
  - Characterising of the fractions by NMR, GPC and DSC.

- Development and evaluation of a solution turbidity fractionation analyser
  - Evaluation of homopolymers to ascertain if the turbidity fractionation analyser can distinguish between different polymers.
- Evaluation of blends by the turbidity fractionation analyser to ascertain possible effects of the homopolymers on each other during solution crystallisation.

The layout of the rest of the thesis is as follows:

### **Chapter 2:**

An overview of the work done in metallocene catalysis, polymerisation and techniques used to fractionate and characterise semi-crystalline polymers

### **Chapter 3**

Summary of the experimental techniques used in this study

### **Chapter 4**

In essence this chapter is an article accepted in the Journal of Applied Polymer Science and discusses the building and development of a solution turbidity fractionation analyser that was built in-house for this research project.

### **Chapter 5**

This chapter focuses on the results obtained for metallocene polymerisation and subsequent characterisation of the homopolymers as well as the blends.

### **Chapter 6**

The conclusions of this study are summarised in this chapter.

## 1.4 References

- (1) Mülhaupt, R. *Macromol. Chem. Phys.* **2003**, *204*, 289-327.
- (2) Harding, G.; Van Reenen, A. J. *Macromol. Chem. Phys.* **2006**, *207*, 1680-1690.
- (3) Lutz, M.; *Relationship between structure and properties of copolymers of propylene and 1-pentene*. PhD Thesis, University of Stellenbosch: Stellenbosch, 2006.
- (4) Shan, C. L. P.; Groot, W. A. D.; Hazlitt, L. G.; Gillespie, D. *Polymer* **2005**, *46*, 11755-11767.

## **Chapter 2**

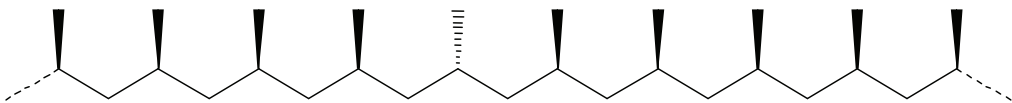
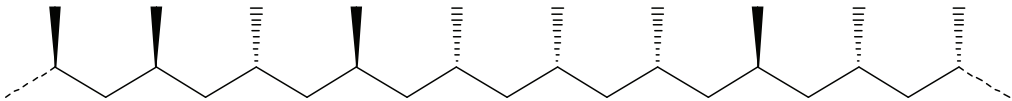
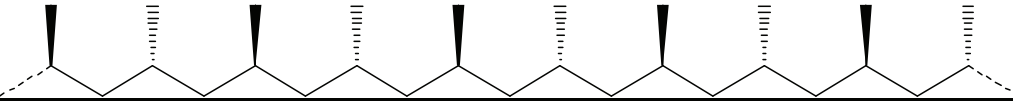
### **Historical Background and Literature review**

*This chapter gives an overview of work done in the field of metallocene catalysis, polymerisation and techniques used to fractionate and characterise semi-crystalline polymers.*

## 2.1 Polypropylene

Polymers are widely used but polyolefins in comparison with other polymers such as polystyrene, polyvinylchloride and polycarbonate, are the most widely used<sup>1</sup>. Polypropylene (PP) is a very useful and versatile polymer and is used daily in any ordinary household. This hasn't always been the case. The use of polymers in household appliances has grown, replacing metals in recent years. Annual world wide total production of polymeric materials has been reported to be approximately 200 million metric tons<sup>1</sup>. Due to the versatility of PP it has grown in popularity. PP can be spun into fibres for use in carpets, bags, rope and even cold-weather gear. PP rope is very popular for use in water sports due to the fact that it is less dense than water and can therefore float. Moulded PP parts are used widely in automotive applications. It is used to make Tupperware®, due to its high melting point it doesn't warp in the dishwasher.

Propylene is a prochiral monomer and as such can insert into a metal-carbon bond during polymerisation in different ways<sup>2</sup>. If we assume that primary insertion occurs, then the enantioface selectivity defines the stereochemistry of each insertion. Multiple insertions of the same enantioface give a polymer with chiral centres in the same configuration, which is defined as an isotactic polymer. Multiple insertions of alternating enantiofaces gives a polymer chain with alternating chiral centres, and is defined as being a syndiotactic polymer. The absence of enantioface selectivity leads to no regularity and atactic polymer results. This is schematically shown in Scheme 2.1.

Name	Polypropylene Structure	Acronym
Isotactic Polypropylene		iPP
Atactic Polypropylene		aPP
Syndiotactic Polypropylene		sPP

**Scheme 2.1:** The three major types of polypropylene tacticities

## 2.2 Metallocene catalysed polymers

The term metallocene is now applied to all catalysts having a single well-defined active center structure, the so-called single site catalysts. According to Resconi et al. group 4 metallocenes are  $d^0$  pseudotetrahedral organometallic compounds in which the transition metal bears two  $\eta^5$ -ligands and 2  $\sigma$ -ligands<sup>2</sup> and is depicted in Figure 2.1<sup>2,3</sup>. The two  $\eta^5$ -ligands are typically cyclopentadienyl (Cp) or substituted Cp ligands.

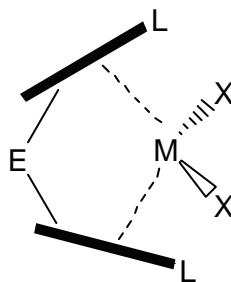
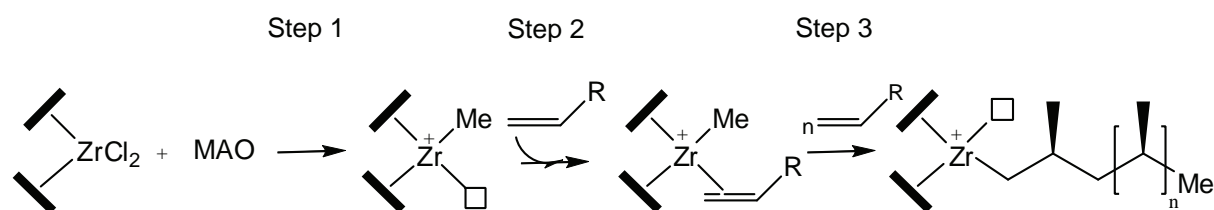


**Figure 2.1:** Generic structure of a metallocene catalyst where Mt is the metal (Ti, Zr, Hf), E is the bridging group ( $R_2C$ ,  $R_2Si$ ,  $-CH_2-CH_2-$ ), X is 2  $e^-$   $\sigma$ -ligand (Cl, Me) and L is a  $\eta^5$  ligand

Breslow and Newburg<sup>4</sup> were first to discover the use of metallocenes as polymerisation catalysts but they used it as a model to study the mechanistic details of Ziegler-Natta catalysis. Metallocenes as polymerisation catalysts for industry became possible when Kaminsky<sup>5</sup> and Sinn<sup>6</sup> discovered that oligomeric methylaluminoxanes (MAO) is a much better cocatalyst than  $Et_2AlCl_3$ <sup>5</sup>. Cocatalysts activate the catalyst by alkylating the transition metal, abstraction of a non-Cp ligand takes place to form active alkyl ion pairs. Cocatalysts also scavenge potential catalyst poisons<sup>5,7,8</sup>. The role of MAO in the activation of a metallocene catalyst is shown in Scheme 2.2. In step 1 the cocatalyst, in this case MAO, undergoes fast ligand exchange with the metallocene dichloride to produce the metallocene methyl and dimethylaluminium compounds and then abstracts either a  $Cl^-$  or  $CH_3^-$  group to produce the metallocene cation and a weakly coordinated MAO anion. The catalyst is now active and has a free coordination position for the monomer. In step 2 the alkene moves into position and in Step 3 the alkene is inserted into the zirconiumalkyl bond rendering a new free coordination site. Step 3 is repeated very quickly, with about 2000 propene molecules inserted per catalyst molecule per second, effectively producing a polymer chain<sup>9</sup>.





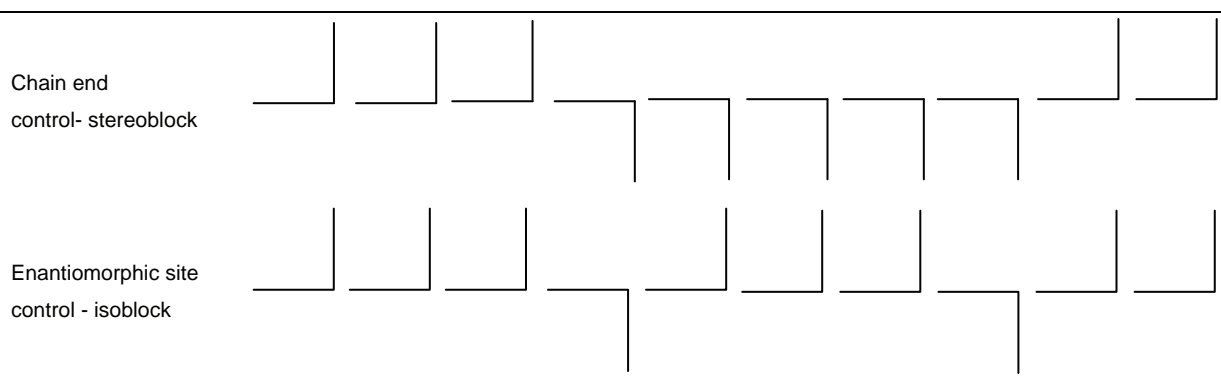
**Scheme 2.2:** The role of MAO in the activation and polymerisation of a metallocene catalyst.<sup>9</sup>

The first iPP polymerisation reaction with metallocene catalysts was performed by Ewen<sup>10</sup>. Commercially PP is mainly produced using conventional heterogeneous Ziegler-Natta catalysts<sup>11</sup>. Heterogeneous transition metal catalysts employed for the production of iPP have active sites that produce only highly isotactic or completely atactic polymer. Producing polymers with varying tacticity is not possible with the heterogeneous transition metal catalysts.

Metallocene catalysts have the advantage that catalyst structure can be varied using synthetic techniques, and that variation in catalyst structures can produce polypropylenes with a wide variety of stereochemistry and molecular weights. For more detail and information I refer to the review by Resconi et al<sup>2</sup>. Random or near random incorporation of comonomer in the production of copolymers is also achieved when using metallocene catalysts.

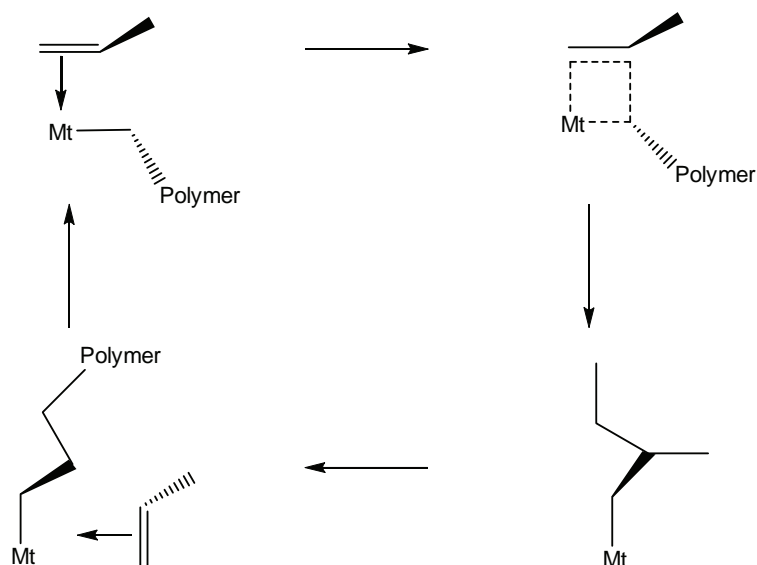
A C<sub>2</sub> symmetric precursor (the symmetry is maintained by the bridge between the Cp ligands effectively blocking their rotation) is necessary to obtain a catalyst that produces isotactic polypropylene. A C<sub>s</sub> symmetric precursor, where the two available coordination positions are enantiotopic, is needed to prepare a catalyst for syndiospecific polymerisation. Asymmetric precursors are used to synthesize metallocene catalysts that produce hemiisotactic and isotactic-stereoblock PP<sup>2,12</sup>. The microstructure of polypropylene is determined by the regio- and stereospecificity of the monomer insertion. To obtain stereocontrol the chirality of the catalytically active species is necessary. In the case of metallocene catalysis the chirality may be located on three parts<sup>2,13</sup>. The elements of chirality needed to obtain stereospecific polymerisation are as follows. The first is the coordination of a prochiral olefin like propylene that gives rise to non-superimposable coordinations, normally depicted as *re* or *si*. This ensures the chirality of the catalyst due to the coordination of the olefin. The second is chirality due to the stereochemistry of the tertiary carbon atom of the last inserted monomer.

Thirdly, there is also the chirality of the catalytic site which can be of two kinds, either the chirality of the coordinated ligands or the chirality of the central atom. These factors all play a role in the way the catalyst controls the stereochemistry of polymerisation. If the coordination of the monomer is directed by the catalyst and is independent of the stereogenic configuration of the last inserted monomer, we refer to the mechanism as enantiomorphic site control. This is the only effective way of controlling stereochemistry. If the configuration of the last inserted monomer controls the coordination of the next monomer the mechanism is called chain end control and is only seen when enantiomorphic site control is absent. Catalysts functioning by chain end control are ineffective and of academic interest only. The type of structures that are obtained for the two mechanisms are depicted in Scheme 2.3. In the case of enantiomorphic site control a misinsertion error is corrected (isolated misinsertion) while with chain end control the error is propagated (This example is for isotactic polypropylene).



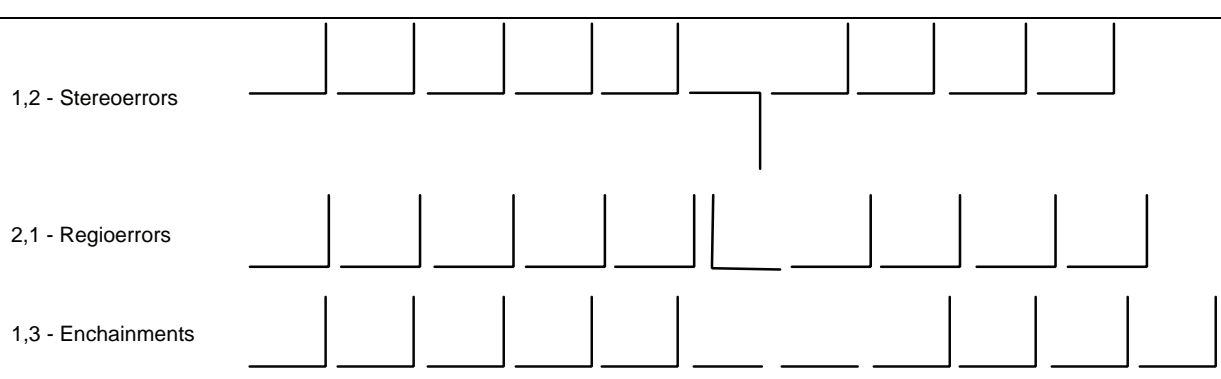
**Scheme 2.3:** Microstructure obtained depending on the stereocontrol mechanism

Polymerisation proceeds by multiple insertions of propylene into a metal-carbon bond. Insertion occurs via the cis-opening of the double bond (both new bonds are on the same side of the inserting propylene) and chain migratory insertion, which means the alkyl groups (polymer chain) on the metal migrate to the propylene. If we have primary or 1,2 insertion, depicted in Scheme 2.4, then the propylene will select the enantioface that will preferentially place the methyl substituent away or anti to the first C-C bond of the growing polymer chain.



**Scheme 2.4:** Primary insertion of propylene into the metal carbon bond

The coordination position of the incoming monomer is determined by the steric influence of the framework. The incoming monomer is positioned by the end of the growing chain that is in turn positioned by the metallocene ligands. Therefore the influence on the monomer is indirect. To obtain isotactic polypropylene (i-PP) insertion of the monomer must be head-to-tail thus 1-2 regiospecific and also stereospecific thus all the methyl bearing carbons must be inserted into the same configuration. Insertion mistakes of the monomer in the main chain can occur but is an isolated event, therefore after the misinsertion occurs the chain will continue as before. Three types of irregularities are found when polymerising metallocene i-PP, namely 1) 1,2-stereoerrors; 2) 2,1-regioerrors and lastly 1,3-enchainments, see Scheme 2.5.



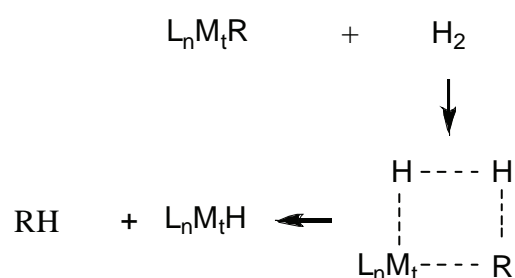
**Scheme 2.5:** Types of errors that can occur during polymerisation of metallocene i-PP

These misinsertions will lead to a decrease in crystallisation with an accompanying decrease in melting temperature due to the disruption in crystal structure.

## 2.3 Molecular weight control in metallocenes

### 2.3.1 Influence of addition of hydrogen to control molecular weight

The use of molecular hydrogen to control molecular weight is used in heterogeneous and metallocene catalysis<sup>2</sup>. The hydrogen level, concentration of monomer, type of catalyst and the reaction temperature influences the degree of molecular weight depression that will occur. After a 2,1 insertion chain growth is terminated by hydrogen and a *n*-butyl end group is formed. The most likely mechanism was found to be the direct insertion of H<sub>2</sub> into the metal-carbon bond, shown in Scheme 2.6.



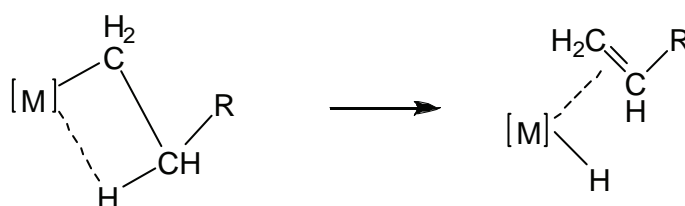
**Scheme 2.6:** The mechanism of direct insertion of H<sub>2</sub> into the metal-carbon bond

In the catalyst system *rac*-Me<sub>2</sub>Si(2-Me-Benz[e]ind)<sub>2</sub>ZrCl<sub>2</sub> (MBI) and *rac*-Me<sub>2</sub>Si(Benz[e]ind)<sub>2</sub>ZrCl<sub>2</sub> the activating effect was limited, only 17% and 38% respectively. A reduction of *n*-butyl end groups was observed and a 6-fold reduction in molecular weight with addition of 0.35 bar H<sub>2</sub><sup>2,14</sup>, in the case of *i*-PP using a MBI/MAO catalyst. The high molecular weight and regioerror reduction shows that the chain release to hydrogen at secondary growth must be much faster than at primary chains.

### 2.3.2 Molecular weight control by means of structural effects

The addition of a linkage between the two Cp rings enabled precise manipulation of the steric environment and from this it was possible to polymerise stereoregular olefin polymers<sup>15</sup>. Changing the bridge length correspondingly changes the Cp-M-Cp angle which has a direct influence on the polymerisation characteristics. The two popular bridges -CH<sub>2</sub>CH<sub>2</sub>- and -Si(CH<sub>3</sub>)<sub>2</sub>- have the same Cp-M-Cp angle but the ethylene bridge allows more relative motion which can lead to decreased molecular weight and stereocontrol in olefin polymerisation relative to the silylene-bridge<sup>16</sup>. Chain termination is the cause of a distribution of molecular

weights. The Schulz-Flory model describes an ideal single site catalyst which produces a polymer with a polydispersity index (PDI) of 2. This limiting value can only be achieved if the rate of chain transfer is relatively larger than the rate of initiation and if there are no reactions that can lead to reactive polymer chain ends or branched polymers. In  $C_2$  symmetric metallocenes the main chain termination reaction is  $\beta$ -hydrogen transfer with the monomer<sup>13,17</sup>. The rate of  $\beta$ -hydride elimination, Scheme 2.7, which directly influences the molecular weight, is dependant on the catalyst used.



**Scheme 2.7:**  $\beta$ -Hydrogen transfer to the monomer in  $C_2$ -symmetric metallocene polymerisation leading to chain termination

Molecular weight control in metallocenes is dependant on the type of ligands used, the nature and position of the substituents on the ligands, the types of bridging groups between the ligands and even the type of metal used. These mechanisms are fairly complex and changes which might improve molecular weight might affect stereocontrol negatively. For the most part, changes which will minimize the amount of 2,1 misinsertions will tend to lead to higher molecular weight<sup>2,8,13,17</sup> polymer. Reaction conditions might also affect the molecular weight. It has been shown that the catalyst concentration has an effect<sup>18</sup>, as does monomer concentration<sup>2</sup>.

## 2.4 Crystallisation of isotactic polypropylene

All polymer crystallisation starts with crystallisation nuclei. Lamellar crystal growth starts at the nuclei. As the lamellae radiate from the central nuclei spherulites are formed if sufficient branching and crosshatching occurs<sup>19</sup>. Nucleation and the growth of polymer crystals at isothermal conditions can best be described by the kinetic nucleation theory<sup>20</sup>. The release of latent heat of fusion, about 210 J/g of crystal, accompanies the crystallisation of PP<sup>19</sup>.

Due to the regularity of iPP it can crystallise. The tacticity of the chain is the main factor that determines the degree of crystallinity<sup>21</sup>. The melting temperature of PP is determined by the average segment length,  $\eta_{iso}$ , and can vary between 120°C and 165°C<sup>1,22</sup>. iPP can assume

different crystalline forms namely  $\alpha$ ,  $\beta$ ,  $\gamma$  and smetic. iPP thus displays polymorphic behaviour<sup>22,23</sup>. The type of crystal that forms is dependant on the nature of the polymer and crystallisation conditions<sup>22</sup>.

The Avrami equation<sup>19</sup>, Equation 2.1 and Equation 2.2, describes the conversion of melt to spherulites during non-isothermal crystallisation.

**Equation 2.1:** The Avrami equation for films

$$\alpha(t) = 1 - \exp\left\{-\pi \int_0^t I(T) \left[ \int_0^t G(s) ds \right]^2 dT\right\}$$

**Equation 2.2:** The Avrami equation for bulk samples

$$\alpha(t) = 1 - \exp\left\{-\left(4 \frac{\pi}{3}\right) \int_0^t I(T) \left[ \int_{L_T}^t G(s) ds \right]^3 dT\right\}$$

Where

$\alpha$  is the overall crystallisation rate

G is the growth rate of the spherulites and

I is the nucleation rate

## 2.5 Molecular weight effects on crystallisation

During fractionation by crystallisation possible molecular weight effects have been ignored in the past. Wild<sup>24</sup> et al. did investigate the possibility of molecular weight effects on TREF. The short chain branching distribution (SCBD) was studied. It was found that at low molecular weights (<10 000 g/mol) there is a significant molecular weight dependence on separation. A calibration curve was used to determine SCBD. Chain ends act as short-chain branches, thus a significant deviation from the calibration was only noted when molecular weight was in the region of 1 000 g/mol. Solvent/non-solvent systems are also used in fractionation experiments. The fractionation of i-PP and polyethylene by solvent/non-solvent systems was investigated by Lehtinen<sup>25</sup> et al. Fractionating with a xylene/ethylene glycol monethyl ether solvent/non-solvent system occurred according to molecular weight for polyethylene. Polypropylene separated according to isotacticity first and then when a constant tacticity was reached, according to molecular weight. Fractionation occurred only according to molecular weight when ethylene glycol monobutyl ether/diethylene glycol

monobutyl ether was used as a solvent/non-solvent system. In the work of Xu<sup>26</sup> et al. characterisation of i-PP polymerised using a supported metallocene catalyst by TREF and various other techniques was investigated. TREF fractionates according to crystallinity and both molecular weight and isotacticity influence crystallinity. It was observed that the viscosity-average molecular weight, of the fractions obtained by TREF, increased with increasing elution temperature. The melting temperature on the other hand only increased in the first seven fractions while staying constant for the last six fractions. From <sup>13</sup>C-NMR it was found that the isotacticity increased in the first seven fractions but stayed constant for the last six fractions. Thus it was concluded that the predominant factor influencing fractionation in the first seven fractions was isotacticity. However, as soon as tacticity stayed constant, as in the case of the last six fractions, molecular weight became the predominant factor influencing crystallinity and thus the fractionation. Lu<sup>27</sup> et al. used TREF as an analytical tool to investigate the effect of isotacticity distribution on the crystallisation and melting behaviour of polypropylene. Three iPP samples ranging in number average molecular weight between 56 000 g/mol and 68 000 g/mol were analysed. The samples were labelled as follow; iPP-56, iPP-57 and iPP-68 where the last two digits represent the magnitude of the number average molecular weight. The isotacticity of the three samples were 93.3%, 93.9% and 95.2% respectively. The molecular weight and isotacticity of these three polymers are approximately the same but differences in crystallisation and melting behaviour were observed. These differences were attributed to differences in their microstructure. In other studies it was proven that the molecular weight of iPP is the predominant factor influencing the growth rate of its crystals under isothermal conditions<sup>28</sup>. It was thus important to ascertain the molecular weight of each fraction obtained from TREF and especially the largest fractions that made up the sample as they will have the biggest influence on the crystallisation. It was found for all three polymers that there were two fractions that made up about 90 wt% of the total polymer. The number average molecular weight of these two fractions for each polymer is summarised in Table 2.1

**Table 2.1:** Summary of the number average molecular ( $\overline{M}_n$ ) weight of the two main fractions of iPP-56, iPP-57 and iPP-68

	<b>iPP-68</b>	
61 000 g/mol		67 000 g/mol
	<b>iPP-56</b>	
35 000 g/mol		133 000 g/mol
	<b>iPP-57</b>	
24 000 g/mol		158 000 g/mol

It was found that iPP-57 had the fastest crystallisation rate while iPP-56 had the slowest. It was concluded that iPP-57 had the fastest crystallisation rate due to its higher nucleation rate. The faster crystallisation rate of iPP-68, in comparison with iPP-56, could be attributed to the relatively small molecular size, of the two main fractions, which increases the reptation motion and thus the overall crystallisation rate. The melting behaviour of the polymers was also affected by the distribution of isotactic elements. It was observed that the iPP-68 had the highest  $T_{mp}$  and  $\Delta H_m$  while iPP-57 had the lowest  $T_{mp}$  and iPP-56 had the lowest  $\Delta H_m$ . A higher  $T_{mp}$  value is an indication of a more perfect crystal structure while the magnitude of  $\Delta H_m$  is a direct measurement of the degree of crystallinity. The higher value of  $T_{mp}$  for iPP-68 can be attributed to a higher ability of reptation motion. This is due to the fact that 90% of the isotactic elements are in the fraction with a  $\overline{M}_n$  of 61 000 g/mol. The molecular chains have more time to rearrange and thus form thicker lamellar crystals. As mentioned previously iPP-56 had the lowest  $\Delta H_m$ , an indication of the degree of crystallinity, this can be explained by the fact that 50% of the isotactic elements for this polymer are situated in the fraction with a  $\overline{M}_n$  of 133 000 g/mol. The bigger molecules decrease reptation motion so the crystals formed are thus thinner and less stable.

Recently the influence of isotacticity and molecular weight on the properties of metallocenic iPP was studied by Arranz-Andrés<sup>23</sup> et al. They concluded that the most important factors affecting the structure and properties of iPP are those that lead to an increase in crystallinity. In a range of polymer samples with the same isotacticity (84%) the sample with low molecular weight showed a significantly higher crystallinity. The crystallisation temperature was higher and the exotherm was narrower, indicating a stronger influence of molecular weight in the crystallisation process. Higher mobility is possible for low molecular weight polymers and crystallisation can thus occur easier. Crystals formed under these conditions should be thinner and thus a lower melting temperature is observed.

## 2.6 Fractionation techniques for semi-crystalline polymers

Classical analytical techniques can provide information on the molecular properties of polyolefins but an average value is obtained and thus no information on the chemical heterogeneity of the sample is obtained. Analytical techniques to study the chemical heterogeneity have been developed during the past several decades. These include temperature rising elution fractionation and crystallisation analysis fractionation.



### 2.6.1 Temperature rising elution fractionation

Temperature rising elution fractionation (TREF) is a well documented technique used for analysis of semi-crystalline polymers. This technique was first used for LDPE and LLDPE<sup>29</sup> and in recent years has moved on to study PP and olefin alloys. Since Shirayma first coined the term and Desreux and Spiegels<sup>30</sup> described the technique, much development has occurred. Fractionation of amorphous polymers using rising temperature will occur according to molecular weight but gel permeation chromatography is commonly used in these cases. Desreux and Spiegels first recognized the potential of using elution at different temperatures to separate semi-crystalline polymers according to crystallisability.

The fractionation mechanism is dependant on differences in the crystallisability of the polymer chain in dilute solution. The thermodynamic equilibrium of a concentrated polymer solution can be described by the Flory-Huggins equation for free energy of mixing. This equation assumes a uniform distribution of solvent and polymer segments. The presence of solvent and the number of chain segments decreases the equilibrium melting temperature of the polymer according to Equation 2.3<sup>31</sup>.

**Equation 2.3:** The Flory-Huggins equation for free energy of mixing

$$\frac{1}{T_m} - \frac{1}{T_m^0} = \left( \frac{R}{\Delta H_u} \right) \left( \frac{V_u}{V_1} \right) \left[ -\frac{\ln(v_2)}{x} + \left( 1 - \frac{1}{x} \right) v_1 - \chi_1 v_1^2 \right]$$

where:

$T_m$  is the equilibrium melting temperature of the polymer in solution

$T_m^0$  is the melting temperature of the pure polymer

$\Delta H_u$  is the heat of fusion per repeating unit

$V_u$  and  $V_1$  are the molar volumes of the polymer repeating unit and diluent respectively

$v_1$  and  $v_2$  are the volume fractions of the diluent and polymer respectively

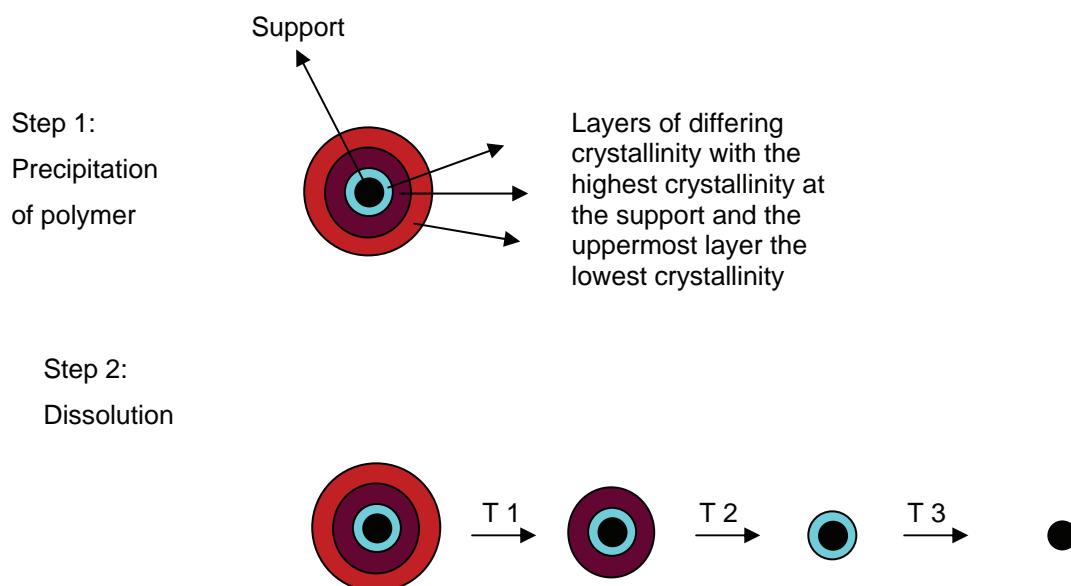
$x$  is the number of segments

$\chi_1$  is the Flory-Huggins thermodynamic interaction parameter

Polypropylene crystallisation is initiated by heterogeneous nucleation. Crystallinity in polypropylene depends on the tacticity or rather the position of the methyl group in relation to the polymer main chain. The nature of the catalyst can influence the stereoregularity along the chain<sup>29</sup>. In the case of metallocene isotactic polypropylene (M-iPP) a small amount

elutes at room temperature and usually a single peak is observed at a higher temperature. M-iPP elutes at lower temperatures in comparison with conventional iPP<sup>32</sup>.

TREF consists of two steps, the first a slow cooling and the second a dissolution step. During the first step the hot polymer solution is cooled at a slow rate (6°C or less per hour) thus resulting in controlled crystallisation. The importance of the cooling step was first recognised by Bergström<sup>33</sup>, Avela<sup>33</sup> and Wild<sup>29</sup>. Rapid precipitation or natural cooling was used in earlier studies. To achieve reproducible separation, based on crystallisability, the crystallisation step must be controlled. Slow cooling of the polymer solution can either occur on a support or in solution. Glass beads, Chromosorb P, silica gel, stainless steel balls and sea sand can all be used as supports<sup>29,34</sup>. The most crystalline polymer crystallises out of solution first, directly onto the support, followed by slightly less crystalline polymer. This continues until the least crystalline polymer (highly branched) crystallises, thus effectively forming the so called onion layers around the support (Scheme 2.8, step 1). In the second step dissolution of the polymer at successively higher temperatures takes place (Scheme 2.8, step 2). The increase in temperature can either be step wise or a continuous temperature gradient.



**Scheme 2.8:** Illustration of the two steps during a TREF experiment

Two types of TREF experiments have been developed over the years namely analytical TREF and preparative TREF (p-TREF). The principles are the same but the main difference is that with p-TREF larger amounts of polymer are fractionated and collected for further

analysis while in analytical TREF no sample collection takes place. In Table 2.2 the two techniques are compared.

**Table 2.2:** Comparison of analytical TREF and p-TREF

<b>Preparative TREF</b>	<b>Analytical TREF</b>
Larger sample sizes needed and thus larger columns needed	Smaller samples and thus smaller columns needed
Fractions are obtained at predetermined temperature intervals	A continuous temperature profile is employed
Further measurements can be obtained off-line (GPC, NMR, DSC etc)	On-line measurement of polymer concentration in solution is measured.
Very time consuming but extra analysis provide much information	Faster than prep-TREF but not as much information is obtained.

### 2.6.2 Turbidity analysis.

According to the International Organisation for Standardization (ISO) turbidity is the reduction of transparency of a liquid caused by the presence of undissolved matter.

In 1966 Imhof<sup>35</sup> recognized the potential of using changes in turbidity to determine the compositional distribution of ethylene homopolymers and blends of ethylene homopolymers and copolymers. A combination of a thermal gradient and a solvent/non-solvent system was utilized to study the change in turbidity. White light from a mercury lamp was used as a light source and the decrease in transmission of the light in the forward direction was measured by a light-scattering photometer. No significant development had occurred until 2005 when Shan<sup>36</sup> et al. published an article describing how the short chain branching distribution (SCBD) of polyethylene can be determined by a turbidimetric method. Changes in the apparatus included the use of a laser diode instead of a mercury lamp. The laser light that passes through the sample cell is monitored by measuring the excitation voltage of the detector. As turbidity increases the amount of laser light that can pass through the solution decreases while the amount of scattering increases. An increase in turbidity occurs when the hot polymer solution is cooled and polymer starts to crystallise out of solution. The reverse of this process leads to the turbidity decreasing with an increase in temperature.

In the article of Shan<sup>36</sup> et al. it was proven that the SCBD can indeed be determined with the turbidity fractionation analyser (TFA). The values obtained was comparable with those from TREF and CRYSTAF. The next step was to explore the quantitative measurement of a

blend. Known weight percentages of a high and low density ethylene-octene polymer were blended. The values obtained from the TFA profiles were very close to the actual values and subsequent runs showed very good reproducibility. A clear dependence on concentration was shown with the low density polymer showing a larger turbidity response than the high density polymer. This means that at the same concentration the lower density polymer blocks more light than the higher density polymer. A possible explanation was that the lower density polymer formed more smaller crystals while the higher density polymer formed larger crystals that are less in comparison. Optical microscopy was used to explain and prove this hypothesis. It was proven that a difference in turbidity response is seen when blends of differing composition were run. Lastly experiments were performed on resins with complicated SCBDs and yet again the TFA was successful in characterising the polymer.

## **2.7 Summary**

This concludes the historical background information and literature review on previous work done on metallocene catalysis and different techniques of characterising semi-crystalline polymers. Even though several techniques already exists to fractionate and characterise semi-crystalline polymers we felt that investigation into the turbidity fractionation analyser is worthwhile for several reasons but one that stands out is the very short analysis time. To fully assess the possible application of the turbidity fractionation analyser it was needed to firstly polymerise polymer with predetermined characteristics and then to fractionate and analyse them. This brings us to the next chapter, namely the experimental aspects of this study followed by the discussion of the results obtained.

## 2.8 References

- (1) Mülhaupt, R. *Macromol. Chem. Phys.* **2003**, *204*, 289-327.
- (2) Resconi, L.; Cavallo, L.; Fait, A.; Piemontesi, F. *Chem. Rev.* **2000**, *100*, 1253-1345.
- (3) Hamielec, A. E.; Soares, J. B. P. In *Polypropylene: An A-Z reference*; Karger-Kocsis, J., Ed.; Kluwer Publishers, 1999; pp 446-453.
- (4) Breslow, D. S.; Newburg, N. R. *J. Am. Chem. Soc.* **1957**, *79*, 5072-5073.
- (5) Ewen, J. A. In *Metallocene-based polyolefins*; Scheirs, J.; Kaminsky, W., Eds.; John Wiley & Sons, Ltd, 2000; Vol. 1, pp 3-31.
- (6) Sinn, H. *Organomet. Chem.* **1980**, *18*, 99.
- (7) Long, W. P. *J. Am. Chem. Soc.* **1958**, *81*, 5312-5316.
- (8) Spaleck, W. In *Metallocene-based polyolefins*; Scheirs, J.; Kaminsky, W., Eds.; John Wiley & Sons Ltd, 2000; Vol. 1, pp 401-424.
- (9) Kaminsky, W.; Laban, A. *Appl. Catal., A* **2001**, *222*, 47-61.
- (10) Ewen, J. A. *J. Am. Chem. Soc.* **1984**, *106*, 6355-6364.
- (11) Ledwinka, H.; Neißl, W. In *Polypropylene: An A-Z reference*; Karger-Kocsis, J., Ed.; Kluwer Publishers, 1999; pp 314-319.
- (12) Mülhaupt, R. In *Polypropylene: An A-Z reference*; Karger-Kocsis, J., Ed.; Kluwer Publishers, 1999; pp 454-475.
- (13) Kaminsky, W. In *Handbook of polymer synthesis*, Second ed.; Kricheldorf, H. R.; Nuyken, O.; Swift, G., Eds.; Marcel Dekker pp 1-72.
- (14) Jüngling, S.; Mülhaupt, R.; Stehling, U.; Brintzinger, H.-H.; Fischer, D.; Langhauser, F. *J. Polym. Sci., Polym. Chem. Ed.* **1995**, *33*, 1305-1317.
- (15) Smith, J. A.; Seyerl, J. v.; Huttner, G.; Brintzinger, H. H. *J. Organomet. Chem* **1979**, *173*, 175-185.
- (16) Piemontesi, F.; Camurati, I.; Resconi, L.; Balboni, D.; Sironi, A.; Moret, M.; Zeigler, R.; Piccolrovazzi, N. *Organometallics* **1995**, *14*, 1256-1266.
- (17) Soga, K.; Uozumi, T.; Kaji, E. In *Metallocene-based polyolefins*; Scheirs, J.; Kaminsky, W., Eds.; John Wiley & Sons, 2000; Vol. 1, pp 381-400.
- (18) Brintzinger, H. H.; Fischer, D.; Mülhaupt, R.; Rieger, B.; Waymouth, R. M. *Angew. Chem. Int. Ed. Engl.* **1995**, *34*, 1143-1170.
- (19) Galeski, A. In *Polypropylene: An A-Z reference*; Karger-Kocsis, J., Ed.; Kluwer Publishers, 1999; pp 135-141.
- (20) Clark, E. J.; Hoffman, J. D. *Macromolecules* **1984**, *17*, 878-885.

- 
- (21) Phillips, R. A.; Wolkowicz, M. D. In *Polypropylene Handbook*; Moore, E. P., Ed.; Hanser Publishers, 1996; pp 113-176.
- (22) Fischer, D.; Jüngling, S.; Schneider, M. J.; Suhm, J.; Mülhaupt, R. In *Metallocene-based polyolefins*; Scheirs, J.; Kaminsky, W., Eds.; John Wiley & Sons, 2000; Vol. 1, pp 103-117.
- (23) Arranz-Andrés, J.; Peña, B.; Benavente, R.; Pérez, E.; Cerrada, M. L. *Eur. Polym. J.* **2007**, *43*, 2357-2370.
- (24) Wild, L.; Ryle, T. R.; Knobloch, D. C.; Peat, I. R. *J. Polym. Sci., Polym. Phys. Ed.* **1982**, *20*, 441-455.
- (25) Lehtinen, A.; Paukkeri, R. *Macromol. Chem. Phys.* **1994**, *195*, 1539-1556.
- (26) Xu, J.; Feng, L. *Eur. Polym. J.* **1999**, *35*, 1289-1294.
- (27) Lu, H.; Qiao, J.; Xu, Y.; Yang, Y. *J. Appl. Polym. Sci.* **2002**, *85*, 333-341.
- (28) Cheng, S. Z. D.; Janimak, J. J.; Zhang, A. *Macromolecules* **1990**, *23*, 298-303.
- (29) Wild, L. *Adv. Polym. Sci.* **1990**, *98*, 1-47.
- (30) Wild, L. *TRIP* **1993**, *1*, 50-55.
- (31) Anantawaraskul, S.; Soares, J. B. P.; Wood-Adams, P. M. *Adv. Polym. Sci.* **2005**, *182*, 1-54.
- (32) Xu, J.; Feng, L. *Eur. Polym. J.* **2000**, *36*, 867-878.
- (33) Bergström, C.; Avela, E. *J. Appl. Polym. Sci.* **1979**, *23*, 163-171.
- (34) Glöckner, G. *J. Appl. Polym. Sci.: Appl. Polym. Symp.* **1990**, *45*, 1-24.
- (35) Imhof, L. G. *J. Appl. Polym. Sci.* **1966**, *10*, 1137-1151.
- (36) Shan, C. L. P.; Groot, W. A. D.; Hazlitt, L. G.; Gillespie, D. *Polymer* **2005**, *46*, 11755-11767.

# Chapter 3

## Experimental

*This chapter focuses on the experimental techniques and analysis that were used to polymerise and characterise the polymer.*

### 3.1 Polymerisation

All equipment used was cleaned beforehand and dried in an oven at 120°C. This includes stainless steel reactors, syringes and Schlenk tubes.

#### 3.1.1 Materials

Propene gas (Aldrich, 99+%), racemic dimethylsilanediyl – bis(2methylbenzo-[e]indenyl zirconium dichloride (MBI, Boulder Scientific company), Methylaluminoxane (MAO, 10 wt.% solution in toluene) and Hydrogen gas (H<sub>2</sub>, Afrox, 99,999%) were used as received. Toluene (Kimix, 99.8%) was dried and distilled under argon gas (Ar, Afrox Scientific UHP Cyl 17.4 kg N5.0, 99.999%) over sodium metal and benzophenone<sup>1</sup> (BP, Sigma, 98%). It was then purged with argon gas and stored in a sealed flask with molecular sieves under argon gas. After polymerisation the reaction solution was precipitated into acidic methanol (10% HCl).

#### 3.1.2 Preparation of the catalyst

A homogeneous catalyst, racemic dimethylsilanediyl – bis(2methylbenzo-[e] indenyl zirconium dichloride ( $\text{rac-Me}_2\text{Si}(2\text{-MeBenz[e]Ind})_2\text{ZrCl}_2$ ) also more commonly known as MBI was used. A standard solution of the catalyst in toluene was prepared. This solution was stored at 4 °C in the dark for a maximum of 5 days. The Al/Zr ratio was kept constant at 2000:1 for all the reactions.

#### 3.1.3 Homogeneous polymerisation of polypropylene

Polymerisation of polypropylene was done using a homogenous metallocene catalyst namely  $\text{rac-Me}_2\text{Si}(2\text{-MeBenz[e]Ind})_2\text{ZrCl}_2$  (MBI). The reaction was done in a stainless steel reactor under a nitrogen atmosphere. A glass insert and magnet was placed into the reactor as soon as it was taken from the oven. It was then closed and cooled under nitrogen gas. The reactor was prepared for reactions by flushing with nitrogen and then evacuating under reduced pressure. The process was repeated four times. To a Schlenk tube, cooled under nitrogen gas and containing a magnetic follower, 1 ml MBI catalyst solution, 3 ml toluene and 3 ml MAO (10% solution in toluene) was added and stirred. In the reactor 20 ml of toluene was added and then the contents of the Schlenk tube were transferred to the reactor. During this process nitrogen continually flowed through the reactor. The addition and transfer of all liquids were done by using a glass syringe and stainless steel needle. The reactor was then



closed. Hydrogen gas was then added by connecting the reactor to the hydrogen cylinder via a stainless steel tube and simply opening the valves and letting it fill the reactor for thirty seconds. The pressure of the hydrogen was controlled by a regulator (Afrox, 101305, 1000 kPa, 230 bar series 9500). Hydrogen gas was used as a transfer agent and thus by changing the pressure of hydrogen gas in the reactor the molecular mass of the polymer could be controlled. Lastly propylene gas was added to the reactor. The reaction mixture was stirred throughout. The reaction time was kept constant at two hours at 25 °C. After two hours the excess polypropylene was vented off, thus effectively stopping the reaction, and the reactor was opened. The reaction solution was then precipitated into acidic methanol (10% HCl) to precipitate the polymer and deactivate the catalyst. The mixture was stirred for two hours to ensure all the polymer precipitated. The solution was then filtered, washed several times with methanol and dried under reduced pressure.

## 3.2 Characterisation

Different techniques were used to characterise the synthesised polymers. This section describes these techniques as well as the sample preparation and conditions needed.

### 3.2.1 High temperature gel permeation chromatography (HT-GPC)

Molecular weights were determined using a PL-GPC 220 high temperature chromatograph (Polymer Laboratories) at 145 °C with a flow rate of 1 ml/min. The columns used were supplied by Polymer Laboratories and packed with a polystyrene/divinylbenzene copolymer (PL gel MIXED-B [9003-53-6]). Samples were prepared in a concentration of 2 mg/ml. The solvent used was 1,2,4 trichlorobenzene (TCB, Fluka, 99.0%) stabilized with 0.0125% 2,6-di-tert-butyl-4-methylphenol (BHT). The BHT was also used as a flow rate marker. The instrument is calibrated using monodisperse polystyrene standards (EasiCal from Polymer Laboratories) and equipped with a differential refractive index detector.

### 3.2.2 Nuclear magnetic resonance (NMR)

<sup>13</sup>C-NMR was performed on all synthesised polymers and selected fractions, obtained from TREF, to determine tacticity. Precise tacticity determination was important and thus a Varian Unity Inova 600 MHz NMR Spectrometer, operating at 150 MHz was used. The method used to collect the <sup>13</sup>C data followed that of Assumption<sup>2</sup> et al. with a 90° pulse width, 1.8 s acquisition time, 15 s pulse delay, and continuous proton decoupling. Spectra were collected

until a sufficient signal-to-noise ratio was achieved (minimum 420 : 1, maximum > 1000). NMR borosilicate tubes were used to prepare the samples. On average, 60 mg of the sample was dissolved at 110°C with deuterated 1,1,2,2 – Tetrachloroethane, (TCE-d<sub>2</sub>, Aldrich, 99.5+ atom % D). Tacticity % determination, mmmm% pentad, was performed according to the rules of Busico et al<sup>3</sup>.

### 3.2.3 Differential scanning calorimetry (DSC)

To determine melting temperature and crystallinity (%) a TA Instruments Q100 DSC system calibrated with indium metal was used. Standard aluminium sample pans were used. Three scans were performed, all at a standard 10 °C/minute rate, for each sample. The samples were first heated to 220 °C and held isothermally for 5 minutes to remove all thermal history. The cooling cycle followed, with the sample cooled to -40 °C and then held at that temperature for 5 minutes. The temperature was then increased to 200 °C for the second heating cycle. The crystallinity (%) was determined from the melting peak on the second heating cycle. The value obtained was divided by 209 J/mol, the theoretical value of 100% crystalline polypropylene, to obtain the percentage crystallinity.

### 3.2.4 Temperature rising elution fractionation analysis (TREF)

This technique, as mentioned in Chapter 2, can either be an analytical technique or a preparative technique. Only preparative TREF (p-TREF) was used in this study. The apparatus was build in-house. Fractionation of homopolymer as well as blends of two homopolymers with difference in molecular weights was done. The polymer was dissolved at 140 °C in TCB with 2% stabiliser (Irganox 1010 and Irgafos 169), relative to the mass of the polymer, added. In the case of the homopolymers, 1 g of sample was dissolved in 150 ml of TCB. The blends required 1 g of each sample and 200 ml of TCB. When the polymer was dissolved it was transferred into a glass reactor. Chromatography grade sea sand, (Sigma-Aldrich, -50 +70 mesh), heated to 140 °C to avoid premature crystallisation, was added to above the level of the solution to assure that no solution crystallisation takes place. The glass reactor was then transferred to an oil bath set at a temperature of 140 °C. The oil bath was then cooled at a controlled rate of 1 °C/hour to 20 °C. The contents of the glass reactor was then transferred to a steel column and heated in a GC-oven in controlled temperature intervals. The polymer was eluted by pumping heated xylene through the column at a controlled rate. A FMI “Q” Pump Model QG150 pump was used and set at a flow rate of 40 ml/min to ensure a constant flow rate.

### 3.2.5 Turbidity fractionation analyser

The turbidity fractionation analyser was built in-house, based on the design of Shan et al<sup>4</sup>. A photo of the experimental setup is shown in Figure 3.1. A more detail description, including a schematic of the instrument, can be found in Chapter 4. A quartz sample holder was used. This fits into an aluminium block mounted on top of a heater/stirrer.

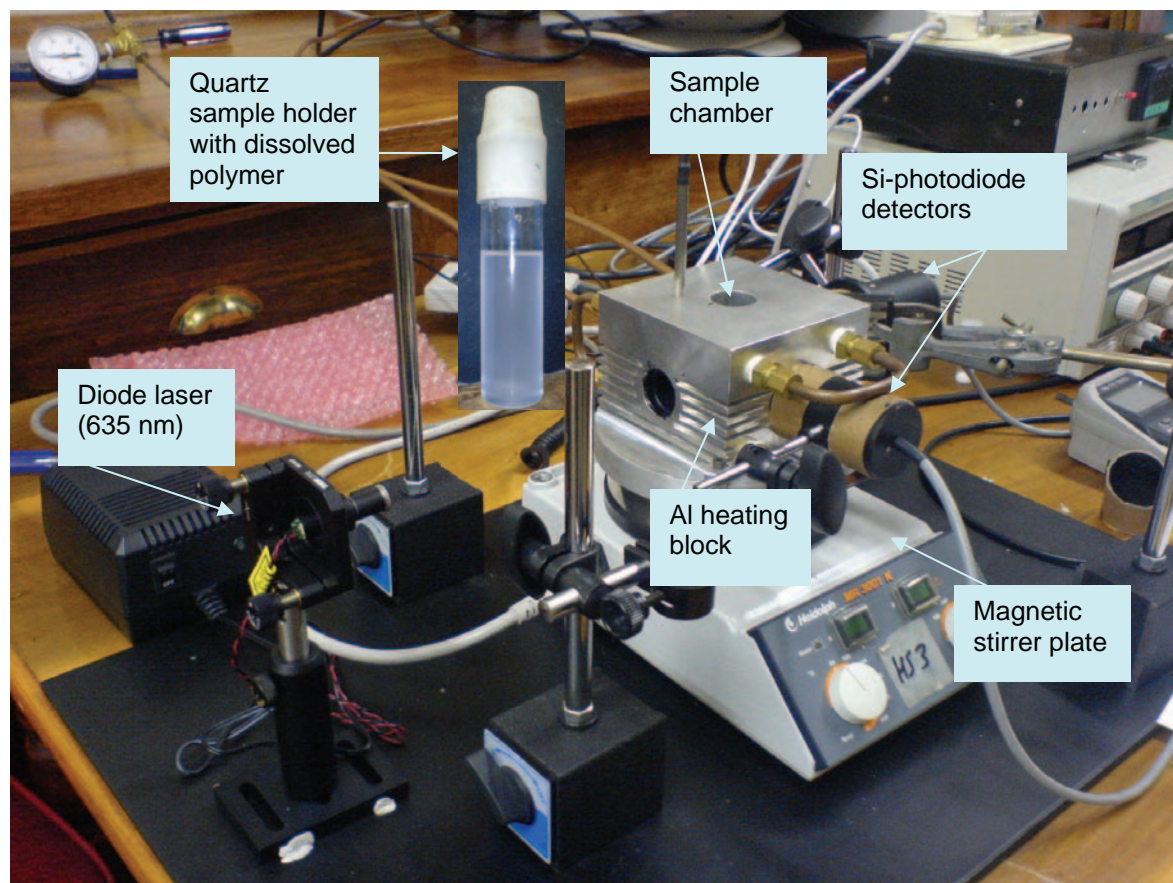


**Figure 3.1:** Experimental setup of the turbidity fractionation analyser

The heater coil is connected to an external temperature controller and together with cooling liquid flowing through the top and bottom of the aluminium block controlled heating and cooling can be achieved. A 4.5 mW Thorlabs diode laser module CPS 196 at 635 nm is used, the laser beam is focused in the centre of the sample cell. Two UDT-555D Si-photodiode detectors were used and placed at angles of 180° and 90° respectively to the laser beam. The detector at 180° measured the change in intensity due to scattering. A neutral density filter was put between the aluminium block and this detector to protect it from saturation. The detector at 90° showed a weaker response which was amplified via the interface. The voltage output of both the photodiode detectors was connected to a Stanford Research Systems SR245 interface and computer for data acquisition. The data acquisition was triggered by a clock pulse of 1 Hz. As said above the heater/stirrer is connected to an

external temperature controller. A microprocessor temperature controller (GEFRAN 800 model) were used to ensure that the temperature, between 30 °C and 100 °C, can be changed, heating or cooling, at a controlled rate, between 0.2 and 2 °C/min. A resistance thermometer probe – Type: PT100 were used as the input from the heater block. Two logic outputs were used, one controlling the hotplate element through a solid state relay and the other regulating the cooling water flow from a cold water tap through the cooling manifold using a solenoid valve switched by a solid state relay. Samples of a concentration of 1 mg/ml in TCB were used, and all samples were heated/cooled at a rate of 1.4 °C/min. The process to optimise the analysis and decide on those parameters is discussed in Chapter 4. A complete discussion of the development of the turbidity fractionation analyser as well as other technical details is given in Chapter 4.

### 3.3 References

- (1) Schwartz, A. M. *Chem. Eng. News* **1978**, *56*, 88.
- (2) Assumption, H. J.; Vermeulen, J. P.; Jarrett, W. L.; Mathias, L. J.; Van Reenen, A. J. *Polymer* **2006**, *47*, 67-74.
- (3) Busico, V.; Cipullo, R.; Monaco, G.; Vacatello, M. *Macromolecules* **1997**, *30*, 6251-6263.
- (4) Shan, C. L. P.; Groot, W. A. D.; Hazlitt, L. G.; Gillespie, D. *Polymer* **2005**, *46*, 11755-11767.

# Chapter 4

## Development of a Turbidity fractionation analyser

*The building and development of a turbidity fractionation analyser that was built in-house for this project is discussed in this chapter.*

This chapter focuses on the building of the turbidity fractionation analyser and on the optimisation of the experimental parameters. The effect of concentration, cooling and heating rate was studied. It is in essence an article accepted for publication in the Journal of Applied Polymer Science.

## 4.1 Introduction

Following the paper published by Shan<sup>1</sup> et al. on the development of a turbidity fractionation analyser, and having at the time of the publication of that paper been in the process of designing a similar piece of equipment, we went ahead and designed and built a system similar in general design to that described by Shan et al. The use of fractionation by crystallisation to study the molecular heterogeneity of polyolefins (for example SCBD) by TREF is well-known and covered by some excellent reviews<sup>2-7</sup>. Similarly, the use of Crystaf, developed by Monrabal<sup>8</sup> for the study of solution crystallisation of polyolefins<sup>6,9,10</sup> is also well-known. We have also used preparative TREF to fractionate polyolefins in several studies<sup>11,12</sup>. The use of a solution turbidity analyser for the study of polyolefin crystallisation behaviour in solution seemed to be a logical step, given the reported short analysis times, as well as the ability to crystallise the polymer from solution, as well as re-dissolving the crystallised material from solution (similar to analytical TREF) in a single experiment<sup>1</sup>. In our case this would be particularly relevant, as we have built up a library of fractionation products of commercial polyolefins, as well as those produced in-house.

## 4.2 Turbidity analyser

The design of our turbidity fractionation analyser used in our experiments to measure the turbidity of polymer solutions, is based on the design published by Shan<sup>1</sup> et al. The schematic of the experimental setup is given in Figure 4.1.

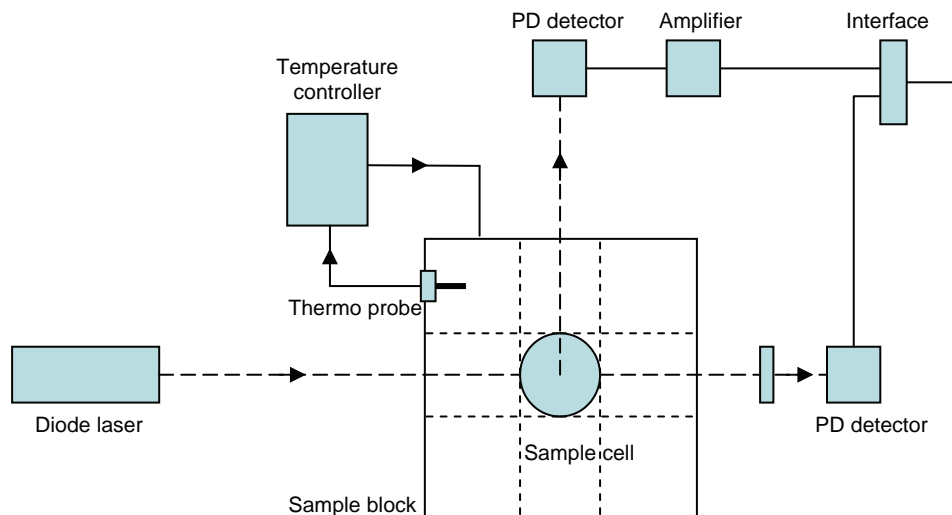


**Figure 4.1:** Schematic diagram of the turbidity fractionation analyser, as viewed from the top.

The quartz sample holder fits tightly into the four-port aluminium block. The aluminium block is mounted on top of a heater/stirrer, of which the heater coil is connected to the external temperature controller. Thermal paste between the heater/stirrer top and the aluminium block ensured maximum thermal contact. Cooling liquid flowing through the top and bottom sections of the aluminium block allows for controlled cooling and heating. The laser beam from a 4.5 mW Thorlabs diode laser module CPS 196 at 635 nm is focused in the centre of the sample cell. For the preliminary experiments two UDT-555D Si photodiode detectors were used to detect scattered light. Each was fitted with a pre-amplifier circuit to boost the signal output. The one photodiode measured the change in the intensity in the forward direction due to scattering. To protect this detector against saturation a neutral density filter was put in the path of the laser. The second detector was mounted at 90° to the laser beam to monitor the changes in scattering caused by the crystallisation of the polymer in the solution with changes in temperature. Because of lower intensity of this signal further amplification is required. Since the diode laser output was quite stable a reference detector was not used in this stage of the investigation. The voltage output of each of the two photodiode detectors was connected to a Stanford Research Systems SR245 interface and computer for data acquisition and handling. The data acquisition was triggered by a clock pulse of 1 Hz.

The inside surfaces of the aluminium block was painted matt black to limit scattering and reflections. Furthermore the interference of room lighting on the detectors was eliminated by tubing between the aluminium block and the detectors.

The temperature control system was designed in-house and offered special features. To change the temperature at a controlled rate (between 0.2 and 2°C/min) in a heating or



cooling range between 30°C and 100°C we used a microprocessor temperature controller (GEFRAN 800 model). As input, from the heater block to control instrument we used a resistance thermometer probe – Type: PT100. Two logic outputs were used, one controlling the hotplate element through a solid state relay and the other regulating the cooling water flow from a cold water tap through the cooling manifold using a solenoid valve switched by a solid state relay.

### 4.3 Chemically distinct polymers

The purpose of the first set of experiments was to see if chemically distinct polymers would give different responses on the instrument, in other words if the technique could distinguish between the crystallisation behaviour of materials which we know to be different. To this end, the materials that were used for analyses and their bulk material properties are listed in Table 4.1.

**Table 4.1:** Characterisation data for the polyolefins used in this study

Polymer	Comonomer (%)	$\overline{M}_w$	PD	Tm (°C)	Crystallinity (DSC)	mmmm%
mPP-1	n/a	35 962	2.7	150.9	81.0	93.8
mPP-2	n/a	65 054	2.2	151.3	70.1	93.3
mPP-3	n/a	141 885	3.1	149.8	55.0	93.5
PP-1-Pent	1-pentene (1.2)	305 800	4.2	151.8	67.4	n/a
LLDPE	1-butene (3.8)	278 340	3.8	122.9	35.9	n/a

mPP = metallocene polypropylene

PP-1-Pent = Propylene-1-pentene copolymer

LLDPE: Linear low density polyethylene (1-butene comonomer)

n/a: Not applicable

A typical response is shown in Figure 4.2. The sharp decrease in the signal from the diode is due to the increased scatter of the incident beam, while the scattered signal at the end of the run is due to the crystallites formed during the process scattering the beam. Data was then analysed with Origin ® software. In order to get a peak, and have the ability to analyse the peak maximum and peak width, the first derivative of the voltage data was calculated. Data was smoothed as the derivative was calculated. A typical result is shown in Figure 4.3

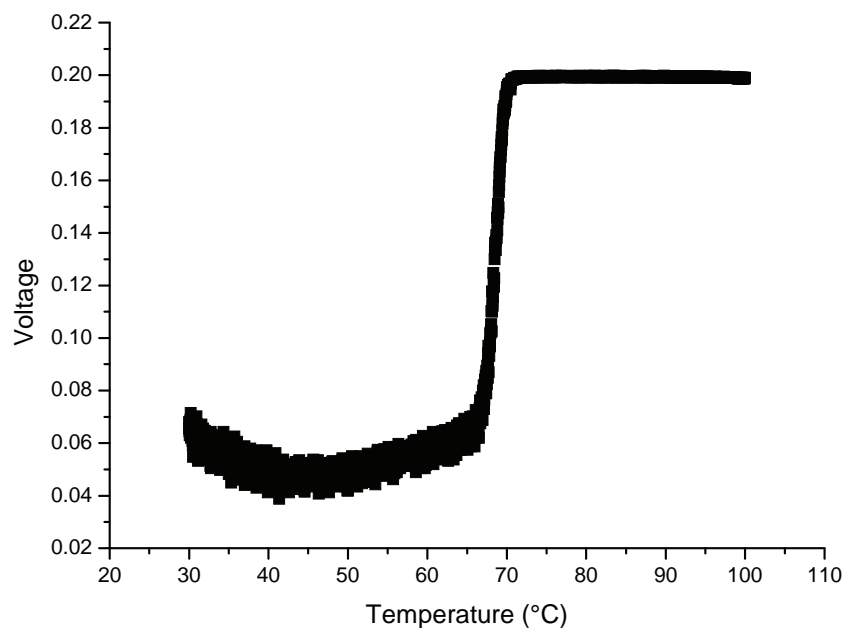


**Figure 4.2:** Raw data, cooling scan of M-iPP-3, 2 °C /minute, concentration of 2 mg/mL, 180° detector.

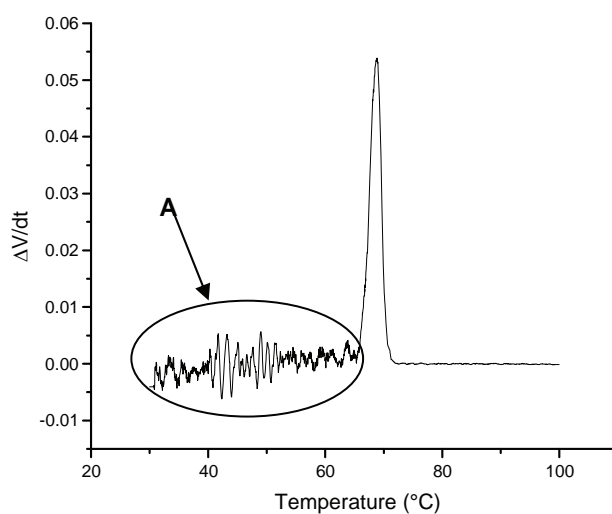


**Figure 4.3:** First derivative of raw data shown in Figure 4.2

In Figure 4.3, extensive scatter after crystallisation is evident (area marked A in the Figure). In other plots presented in this paper, extensive smoothing of data in this area was done before taking the first derivative. This was done in order to be able to present overlays of different sets of results.

As mentioned, initial experiments were conducted to see if we could differentiate between chemically different polymers. To this end, we compared three polymers, a commercial LLDPE (comonomer 1-butene (6 mole%)), a polypropylene-1-pentene copolymer (1.2 mole% comonomer) and a polypropylene prepared with a metallocene catalyst (mPP-3). In each case a cooling rate of 2°C /minute was used, and a polymer concentration of 2 mg/mL. An overlay of two of the scans, that of the LLDPE and the PP-1-pentene copolymer is shown in Figure 4.4. Comparing this scan for mPP-2 (Figure 4.3) we can see that the crystallisation behaviour of the three polymers is different, not only with respect to the peak crystallisation temperatures, but also with respect to the range over which crystallisation occurs. In particular, the set of conditions selected for the LLDPE lead to a very broad peak, with the scattering having a severe influence on the ability to isolate and identify the crystallisation peak.

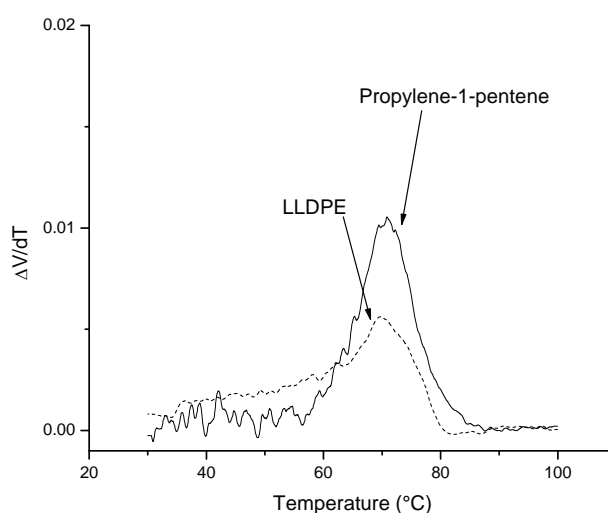


**Figure 4.4:** Comparison of a propylene-1-pentene copolymer and LLDPE analyzed under identical conditions (2 mg/mL, 2 °C/min).

## 4.4 Effect of experimental parameters

### 4.4.1 Sample concentration effects

The initial experiments indicated that the crystallisation behaviour seems to be dependent on experimental parameters. This would include concentration of the polymer in solution and cooling rates. The concentration not only affects the peak crystallisation temperature (determined from the first derivative plot), but also the scatter and range of crystallisation. The latter is illustrated in Figure 4.5, where we illustrate the effect of sample concentration on

the crystallisation profiles of a commercial propylene-1-pentene copolymer. Two solutions, one of 2 mg/mL and one of 0.5 mg/mL were compared.

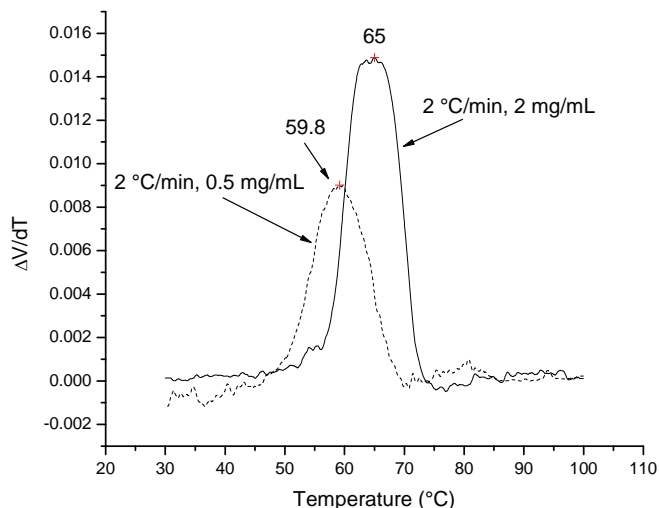


**Figure 4.5:** Concentration effects during crystallisation from solution for a propylene-1-pentene copolymer.

From Figure 4.5 it can be seen that the higher the concentration, the higher the crystallisation temperature, for a given cooling rate. Intuitively this is to be expected, as a higher concentration of polymer will lead to more rapid crystallisation. It is also noticeable that the peak width for the crystallisation of the polymer with the lower concentration is wider than that of the solution with the substantially higher concentration.

#### 4.4.2 Cooling rate

It was expected that the cooling rate could play a role in the data generated by these experiments. As one of the big advantages with these experiments is seen to be the fairly short scan times, we felt it necessary to see how big an effect the cooling rate has on the results. For example, in Figure 4.6 we illustrate the difference achieved in when comparing cooling rates of 2, 1.4 and 1 °C/minute.

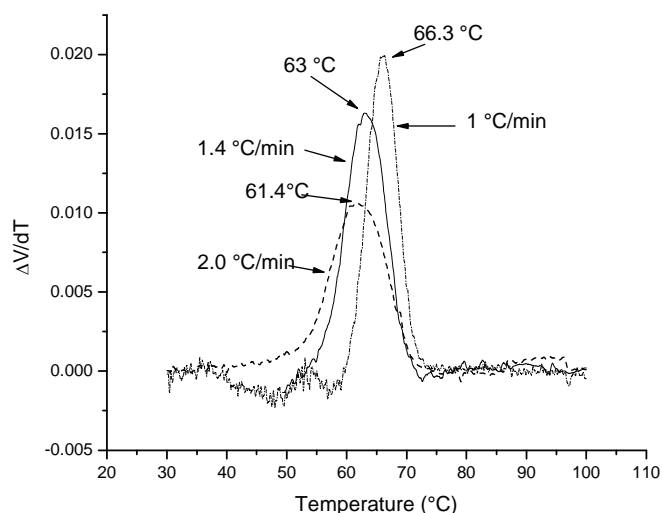


**Figure 4.6:** The effect of cooling rate on the crystallisation of PP-1-Pentene. Cooling rates of 1, 1.4 and 2 °C were used. The solution concentration was 1 mg/mL.

Even with a relatively small change in the cooling rate, we see a significant change in the peak temperature of the first derivative peaks of the cooling profiles for three solutions (1 mg/mL) of the propylene-1-pentene copolymer. The peak width of the slower cooling rate is less than that of the slightly faster cooling rate, while the crystallisation range also appears to be narrower when the cooling rate is decreased. Unfortunately the data capture package used for these experiments precluded utilising even slower cooling rates.

#### 4.4.3 Heating rate

It is obvious that the reverse of the cooling experiments can be done. The suspension of crystallised material can be heated and the disappearance of scattering can be recorded, and upon derivation and smoothing a heating curve can be obtained. In Figure 4.7 the results of the heating experiments of similar solutions of a propylene-1-pentene copolymer are shown.

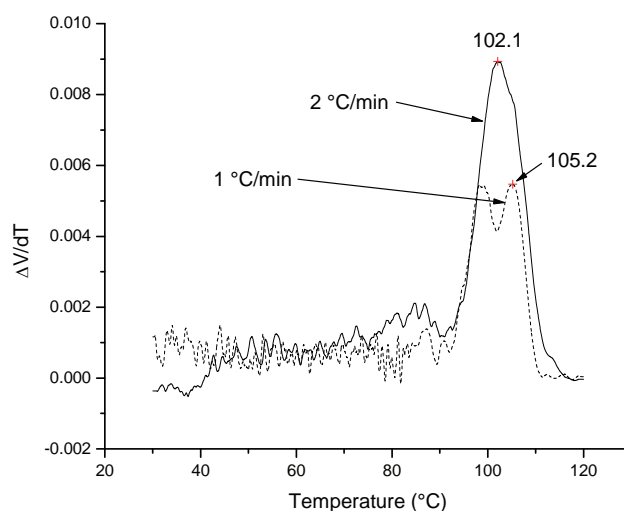


**Figure 4.7:** The heating profiles of 1 mg/mL solutions of a PP-1-pentene copolymer. Heating rates of 1 and 2 °C/minute are shown.

In Figure 4.7 the dashed line represents the first derivative of the heating curve of a solution of 1 mg/mL of the propylene-1-pentene copolymer heated at 1 °C/min, while the solid line represents the 2 °C/min experiment. The peak with an apparent shoulder of the crystallised material heated at 2 °C/min is clearly resolved into two maxima when the material is heated at 1 °C/min. It is possible that some more peaks might be present at lower temperatures, but the amount of scatter makes it impossible to make statements in this regard. Similar experiments conducted at 3.5 °C/min yielded a very broad peak with a severe tailing towards higher temperatures.

#### 4.4.4 Molecular weight effects.

As an additional experiment, we synthesized three metallocene copolymers with the same metallocene catalyst, keeping the catalyst/cocatalyst/monomer ratio constant for all three reactions, while varying the amount of hydrogen introduced into the reaction. Tacticities are given in Table 4.1. It is clear that the two polymers have very similar tacticities, while the molecular weight of the two materials is quite different. The overlay of the crystallisation experiment is shown in Figure 4.8. In this case it is clear that a molecular weight effect appears to be present during the solution crystallisation of the polymers. This is significant, as molecular weight effects are generally ignored during fractionation by crystallisation experiments. The effect of molecular weight on the fractionation was considered by Wild<sup>13</sup>. The data obtained by Wild indicated that if the polymer chain ends are considered to be the equivalent of a branch point then the molecular weight dependence on the fractionation

mostly disappears. They also showed that the molecular weight dependence falls away as soon as the molecular weight reaches approximately  $10^4$  g/mol.

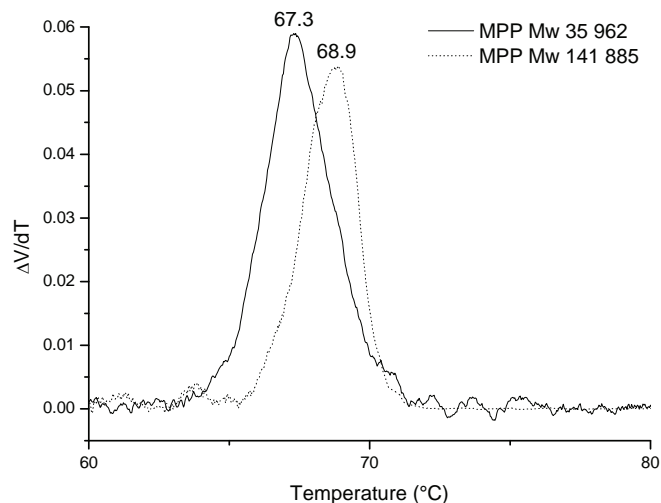


**Figure 4.8:** Crystallisation profiles of two polypropylenes prepared by a metallocene catalyst.

The dashed line represents the polymer with a molecular weight of 141 885, while the solid line represents a polymer with a molecular weight of 35 962. Sample concentration was 2 mg/mL and cooling rate 2 °C/min.

The optimisation of the instrument was needed to decide the best experimental parameters that will be used further in the study. Based on these preliminary experiments it was decided that the optimum concentration for the metallocene polymers is 1mg/ml at a cooling rate of 1,4 °C/min. It was decided to concentrate only on the cooling experiments further and thus in Chapter 5 all the TFA data are of cooling with the formerly mentioned parameters.

## 4.5 References

- (1) Shan, C. L. P.; Groot, W. A. D.; Hazlitt, L. G.; Gillespie, D. *Polymer* **2005**, *46*, 11755-11767.
- (2) Wild, L. *Adv. Polym. Sci.* **1990**, *98*, 1-47.
- (3) Soares, J. B. P.; Hamielac, A. E. In *Modern Techniques for Polymer Characterisation*; Pethrick, R. A.; Dawkins, J. V., Eds.; John Wiley & Sons: Chichester, 1999; pp 15-55.
- (4) Xu, J.; Feng, L. *Eur. Polym. J.* **2000**, *36*, 867-878.
- (5) Glöckner, G. *J. Appl. Polym. Sci.: Appl. Polym. Symp.* **1990**, *45*, 1-24.
- (6) Monrabel, B. In *Encyclopedia of Analytical Chemistry*, 2000; Vol. 9, pp 8074-8094.
- (7) Soares, J. B. P.; Hamielec, A. E. *Polymer* **1995**, *36*, 1639-1654.
- (8) Monrabel, B.: US Patent 5 222 390, 1991.
- (9) Monrabal, B. *J. Appl. Polym. Sci.* **1994**, *52*, 491-499.
- (10) Monrabel, B. *Macromol. Symp.* **1996**, *110*, 81-86.
- (11) Harding, G.; Van Reenen, A. J. *Macromol. Chem. Phys.* **2006**, *207*, 1680-1690.
- (12) Assumption, H. J.; Vermeulen, J. P.; Jarrett, W. L.; Mathias, L. J.; Van Reenen, A. J. *Polymer* **2006**, *47*, 67-74.
- (13) Wild, L., Ryle, T.R., Knobloch, D.C., & Peat, I.R. *J. Polym. Sci.: Polym. Phys. Ed.* **1982**, *20*, 441-455.



# Chapter 5

## Results and Discussion

*This chapter summarises the results obtained for metallocene polymerisation, blending and characterisation of the polymers*

## 5.1 Characterisation of the metallocene isotactic polypropylene homopolymers

### 5.1.1 The unfractionated metallocene homopolymers

Complete characterisation of the homopolymers was needed before any further experiments were performed. The next step was creating blends consisting of two homopolymers where the tacticity is the same but the molecular weight differs. The most important information thus needed was the tacticity (%) and molecular weight data. NMR analyses were performed on all the homopolymers but to avoid repetition one spectrum representative of all the homopolymers is showed in Figure 5.1. The tacticity, indicated by the peaks due to stereoerrors, next to the CH<sub>3</sub> peak, is difficult to see when the whole spectrum is shown. For clarity that section is zoomed in and shown as an insert on Figure 5.1. As mentioned in section 3.2.2 isotacticity was calculated according to the procedure of Busico<sup>1</sup> et al. and showed in Table 5.1.

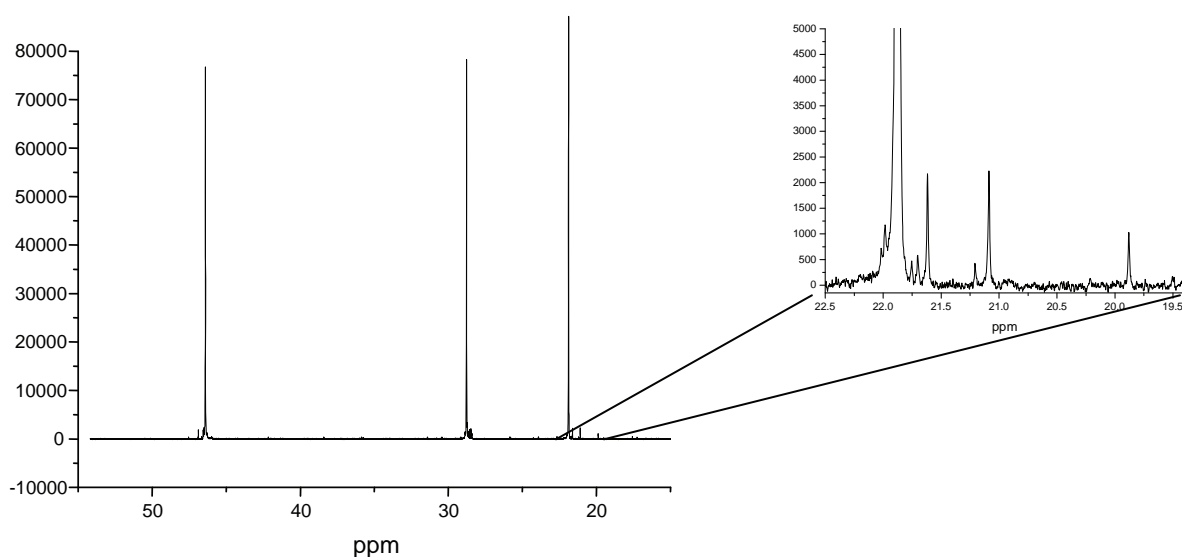


**Figure 5.1:** NMR spectrum of M-iPP1 with insert of isotactic peaks

The next important information needed was the molecular weight data. In Table 5.1 the GPC data as well as the isotacticity determined from NMR is summarised.

**Table 5.1:** Summary of  $\overline{M}_w$ ,  $\overline{M}_n$ , melting temperature and crystallinity of metallocene i-PP

Sample Name	$\overline{M}_w$	$\overline{M}_n$	PDI	Isotacticity (%)	Hydrogen (%)
M-iPP-1	68185	32283	2.11	93.78	0.16
M-iPP-2	68772	12038	5.71	95.82	0.15
M-iPP-3	38506	12554	3.06	92.72	0.68
M-iPP-4	35328	17541	2.01	96.55	0.70
M-iPP-5	83593	20138	4.15	93.26	0.00
M-iPP-6	134984	46380	2.91	93.35	0.00

In the case of samples M-iPP-2 and M-iPP-5 we see a very broad molecular weight distribution. This is uncommon for metallocene catalyzed polypropylene. All discussions regarding the use of these two samples in blending experiments should take these characteristics into account. In addition to the molecular weight and tacticity data presented in Table 5.1, the results of the DSC analyses are shown in Table 5.2.

**Table 5.2:** Summary of the DSC data for the homopolymers.

Sample Name	% Crystallinity	Melting Temperature (°C)	T <sub>c</sub> (°C)
M-iPP-1	70.00	153.65	116.51
M-iPP-2	47.99	146.80	110.36
M-iPP-3	54.69	148.72	115.15
M-iPP-4	62.92	153.09	118.39
M-iPP-5	58.56	146.27	111.78
M-iPP-6	54.97	149.83	112.91

T<sub>c</sub> Crystallisation temperature

If we look at the DSC melting temperature values for these polymers we see they are all in the range 146 – 153 °C, while tacticity values vary between 92.7% and 96.6%. The rule of thumb, for isotactic polypropylene prepared with heterogeneous catalysts, is that tacticity is directly related to the melting temperature. This is not the case for these metallocene polymers. Take for example M-iPP-1 and M-iPP-4, with melting temperatures of 153.7 and 153.1 °C respectively. Within experimental error, these are essentially identical. Yet the tacticities are 93.8 and 96.6%. These polymers have crystallinity values of 70% and 63%, with the higher crystallinity being associated with the polymer with the lowest tacticity. The only notable difference between these polymers is the molecular weight, with M-iPP-1 having roughly double the molecular weight of M-iPP-4. This could be taken as an indication that molecular weight could play a role in crystallisation in the bulk. There could, of course be other factors involved, like the amount of 2, 1 insertions in the polymer chain. These could

disrupt crystallinity quite considerably, and would not interfere with the measurement of tacticity, as monomers that undergo 2, 1 insertions show up on a different area of the  $^{13}\text{C}$  NMR spectrum than that used for the calculation of tacticity. In the  $^{13}\text{C}$  NMR spectrum of M-iPP-5 the 2, 1 and 3, 1 insertions, illustrated with a hash (#), can be seen clearly in Figure 5.2. Different types of end-groups, illustrated with a star (\*), are also shown.

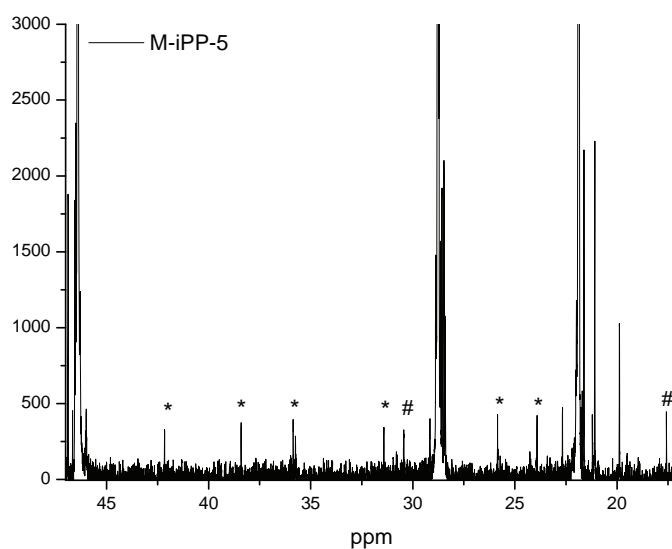


**Figure 5.2:**  $^{13}\text{C}$  NMR spectrum showing 2,1 and 3, 1 insertions as well as different endgroups of M-iPP-5

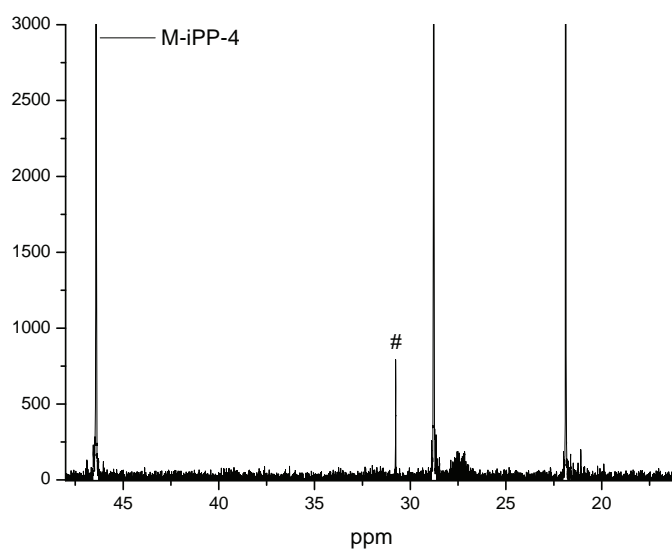


**Figure 5.3:**  $^{13}\text{C}$  NMR showing the 2,1 insertions in M-iPP-4

It is also possible that with some of these polymers, catalyst isomerisation during polymerisation could lead to two different active species, with a resultant mixture of atactic and isotactic polymers, with a broad molecular weight distribution. This could influence the measurement of overall tacticity and crystallinity. It is noticeable that the two polymers with the broadest molecular weight distribution have the lowest melting temperatures, even though the tacticity values are comparable with the other polymers.

### 5.1.2 The fractionated metallocene homopolymers

The homopolymers were fractionated by prep-TREF to obtain individual fractions for further analysis. Figure 5.4 shows the TREF overlays of the homopolymers. The amount of polymer for each experiment was not the same and so, to be able to make a direct comparison between experiments, the weight fraction percentages ( $W_i\%$ ) was taken. Weight fraction percentage is the amount of polymer collected at the fractionation temperature divided by the total amount of polymer collected in the run, and presented as a percentage. A distinct room temperature fraction and a large high temperature fraction are observed. This is unexpected, as most metallocene catalyzed polymers are supposed to be homogeneous. From Figure 5.4 it can be seen that the temperature at which the major fractions elutes is between 100°C and 110°C even though all samples are metallocene isotactic polypropylene. The three polymers that have the major fraction eluting at 110 °C are three materials with higher molecular weight and the narrowest polydispersity. A lower PDI suggests a more homogeneous polymer in regards to length and thus a polymer that will crystallise easier and subsequently elute at a higher temperature. At the same time the narrow PDI indicates less low molecular weight material which might interfere with the crystallisation process.

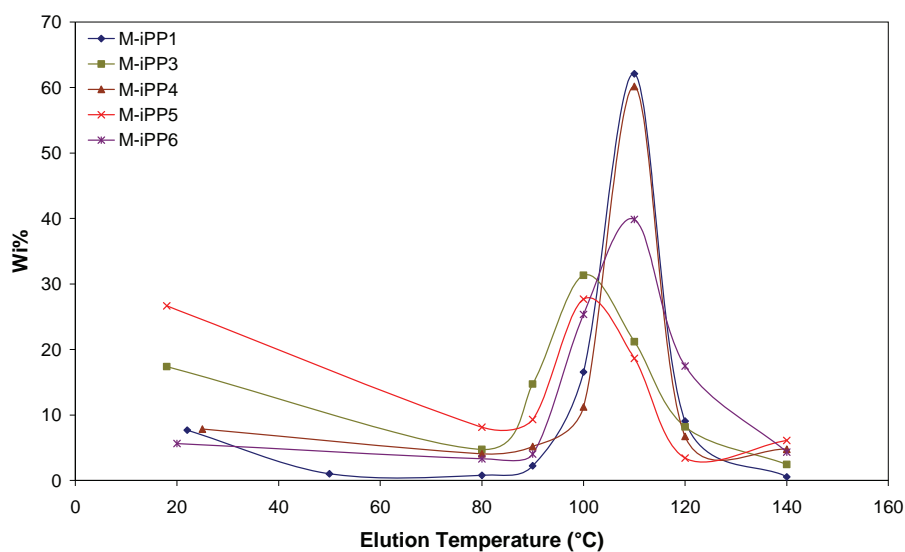


**Figure 5.4:** TREF overlay of the homopolymers

The peak width of the TREF profiles also differs. The narrowest peak width is obtained when the polymers' PDI is low. In practical terms, the wider the peak width, the broader the molecular species distribution in the polymer. Crystallisation occurs over a broader temperature range. In the case of these polymers, this molecular species distribution appears to be greater with a higher PDI. The three polymer samples with broader peak widths have a PDI of 3 and higher. M-iPP 2 is missing in Figure 5.4, after the polymer were used in the blending experiment not enough was left over for a homopolymer fractionation experiment.

**Table 5.3:** Summary of the GPC data of the fractionated homopolymers

Elution Temperature (°C)	$\overline{M}_w$	$\overline{M}_n$	Weighted Fraction (%)	Mass (g)	PDI
<b>M-iPP-1</b>					
22	13703	7580	7.69	0.07	1.8
80	10228	3278	0.78	0.01	3.12
90	20552	10932	2.23	0.02	1.88
100	64109	30348	16.56	0.14	2.11
110	73517	41684	62.10	0.53	1.76
120	72907	41294	9.07	0.08	1.76
140	n/e	n/e	0.55	0.00	n/a
<b>M-iPP-3</b>					
<b>18</b>	4294	324	17.38	0.21	13.25
<b>80</b>	4316	2917	4.74	0.06	1.47
<b>90</b>	9259	5242	14.72	0.18	1.76
<b>100</b>	25370	12087	31.32	0.38	2.09
<b>110</b>	24262	11853	21.19	0.26	2.05
<b>120</b>	20028	10199	8.19	0.10	1.96
<b>140</b>	29416	12475	2.45	0.03	2.35
<b>M-iPP-4</b>					
25	14965	9314	7.84	0.11	1.61
80	4106	363	4.07	0.05	11.31
90	11587	5892	5.19	0.07	1.96
100	19817	10458	11.23	0.15	1.89
110	35734	20195	60.18	0.81	1.77
120	19058	10321	6.74	0.09	1.85
140	27705	7303	4.75	0.06	3.79
<b>M-iPP-5</b>					
<b>18</b>	19662	18166	26.66	0.29	1.08
<b>80</b>	6106	3443	8.14	0.09	1.77
<b>90</b>	13324	7088	9.30	0.10	1.87
<b>100</b>	35063	16050	27.69	0.30	2.18
<b>110</b>	28117	13448	18.66	0.20	2.09
<b>120</b>	23847	12084	3.43	0.04	1.97
<b>140</b>	23601	8617	6.12	0.07	2.73
<b>M-iPP-6</b>					
<b>20</b>	3667	3666	5.64	0.05	1.00
<b>80</b>	12937	5947	3.30	0.03	2.18
<b>90</b>	25742	11805	4.01	0.03	2.18
<b>100</b>	82098	32754	25.36	0.23	2.51
<b>110</b>	114570	44389	39.85	0.36	2.58
<b>120</b>	48428	21184	17.48	0.15	2.29
<b>140</b>	38824	15344	4.33	0.03	2.53

n/e not enough sample for analysis

The original goal of the research was to investigate the effect of molecular weight on crystallisation during preparative and analytical experiments. Even though it was apparent from the TREF results that these polymers were not as homogeneous as we had hoped, blends were made of the homopolymers. The blends, 50/50 by mass, consisted, for example, of two homopolymers differing significantly in molecular weight but with roughly the same isotacticity for the bulk sample. In other cases materials with similar molecular weights but different tacticities were blended. The material was solution blended during the experiment. TREF experiments were performed on four such blends. In Figure 5.5 the overlay of the four TREF experiments are shown. The main peak for three of the blends eluted at 100 °C, whereas the main peak for the M-iPP 1+4 blend eluted at 110 °C. When this result was compared with the TREF runs of the original individual polymers (M-iPP 1 and M-iPP 4) it was seen that for both the original samples the main fraction eluted at 110 °C. In the case of blend M-iPP 3+4 the main fraction eluted at 100 °C while the main fraction obtained with TREF for the original polymers eluted at 100 °C and 110 °C respectively.

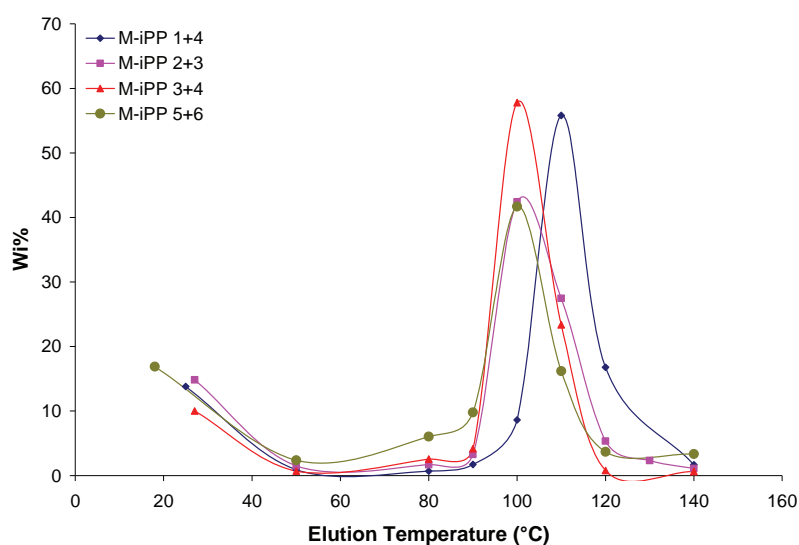


**Figure 5.5:** TREF overlay of the blends

Explanation of shifts in the TREF profiles can't be explained by only comparing bulk sample values. Characterisation of the individual fractions was needed. Due to limited amounts of polymer obtained for certain fractions after fractionation full characterisation of each fraction was not possible. Only the larger fractions which are the most important when looking at bulk properties were fully characterised. Fractionation and thereafter characterisation of the individual fractions was performed not only on the blends but also on the individual polymers. During crystallisation the main influence is crystallisability of the samples. Molecular weight



and tacticity are the two factors that influence the crystallisability of a sample. The effect of molecular weight on crystallisation has largely been ignored in the past as it was said that it only has an effect below 10 000 g/mol<sup>2</sup>. Recently, a critical investigation into this statement has occurred<sup>3-5</sup>. It has become clear that even though molecular weight isn't necessarily the major factor during crystallisation it cannot be ignored in its entirety.

During fractionation stereoregularity is the foremost factor influencing fractionation. However, when the difference in stereoregularity ceases to exist between fractions, molecular weight takes over<sup>4,5</sup>. Similar stereoregularity is important when choosing appropriate homopolymers for blending studies, but the stereoregularity as calculated was that of the bulk. Therefore we also conducted <sup>13</sup>C NMR analyses of the fractions that eluted at 100 °C and 110 °C to determine the isotacticity distribution (if any) in the crystalline fraction of the polymers. Results are summarised in Table 5.4 for the individual polymers and in Table 5.5 for the blends.

**Table 5.4:** Isotacticity of the individual samples obtained by TREF

<b>M-iPP 1</b>	
<b>TREF Fraction</b>	<b>mmmm%</b>
100°C	93.07
110°C	93.61
<b>M-iPP 4</b>	
100°C	94.97
110°C	89.18
<b>M-iPP 5</b>	
100°C	87.89
110°C	92.41
<b>M-iPP 6</b>	
100°C	90.5
110°C	89.41

It is noticeable that in the cases of polymers 1 and 6, those with the highest molecular weight, the distribution of tacticity over the crystalline fractions are very similar, while for the other two polymers there appears to be a distinct difference in the tacticity values. In addition, the molecular weight of the fractions for polymer 1 and 6 are higher for the 110 °C fractions than for the 100 °C. So it appears as if molecular weight is the dominant factor determining the crystallisation behaviour here. On the other hand, for polymer 4, the tacticity for the 110 °C fraction is lower than for the 100 °C fraction, but the molecular weight is

almost double that of the 100 °C fraction. So in this case the molecular weight once again appears to be the dominant factor. In the case of polymer 5, the molecular weights of the two fractions are much closer together, and the dominant factor determining the crystallisation is the tacticity.

**Table 5.5:** Isotacticity of the TREF fractions of the blends

<b>M-iPP 2+3</b>	
<b>TREF Fraction</b>	<b>mmmm%</b>
100°C	90.61
110°C	92.81
<b>M-iPP 3+4</b>	
100°C	95.34
110°C	98.98
<b>M-iPP 5+6</b>	
90°C	85.83
100°C	83.83
110°C	89.22

Molecular weight data, crystallisation temp, melting temperature and percentage crystallinity was determined for selected fractions as well and is summarised in Table 5.6.

**Table 5.6:** GPC and DSC data of the fractionated blends

Elution Temperature	$\overline{M_w}$	$\overline{M_n}$	PDI	Weighted Fraction (%)	Mass (g)	Melting Temp	T <sub>c</sub>	Crystallinity %
<b>M-iPP 2+3</b>								
27°C	372	257	1.44	14.84	0.27	n/d	n/d	n/d
80°C	8772	5177	1.70	1.69	0.03	136.08	106.07	46.95
90°C	19870	10610	1.87	3.28	0.06	142.93	110.81	69.18
100°C	60474	27686	2.18	42.42	0.78	147.86	111.96	49.86
110°C	62428	30177	2.07	27.47	0.51	150.05	113.61	66.6
120°C	45408	21918	2.07	5.36	0.10	149.86	112.1	26.22
130°C	n/e	n/e	n/e	2.34	0.04	146.42	113.14	4.24
140°C	n/e	n/e	n/e	1.10	0.02	140.29	106.29	4.09
<b>M-iPP 1+4</b>								
24°C	16563	23212	1.4	13.80	0.31	n/d	n/d	n/d
80°C	5763	2250	2.56	0.68	0.02	129.23	98.49	33.12
90°C	17688	7622	2.32	1.73	0.04	146.61	107.46	46.18
100°C	34170	15134	2.25	8.63	0.20	149.23	113.06	42.82
110°C	55825	27417	2.03	55.80	1.27	152.68	114.71	67.99
120°C	57149	30017	1.9	16.78	0.38	152.88	115.67	40.04
140°C	100263	32524	3.08	1.66	0.04	n/e	n/e	n/e
<b>M-iPP 3+4</b>								
27°C	49748	20200	2.46	10.00	0.18	n/d	n/d	n/d
80°C	7871	5379	1.46	2.55	0.05	140.72	108.55	46.69
90°C	16049	10551	1.52	4.17	0.07	147.08	112.5	37.14
100°C	56316	29757	1.89	57.80	1.03	153.03	115.48	54.06
110°C	58503	31871	1.83	23.36	0.42	153.08	115.35	50.28
120°	59648	30346	1.96	0.80	0.01	n/e	n/e	n/e
140°C	84091	27191	3.09	0.63	0.01	n/e	n/e	n/e
<b>M-iPP 5+6</b>								
18°C	15997	7787	2.05	16.90	0.43	n/e	n/e	n/e
80°C	10060	5186	1.93	6.04	0.15	128.19	97.05	28.06
90°C	21893	10630	2.05	9.79	0.25	138.5	105.45	27.92
100°C	80896	30367	2.66	41.69	1.06	146.02	108.71	45.87
110°C	53248	22599	2.35	16.21	0.41	145.9	110.07	42.62
140°C	29957	5049	5.93	3.34	0.08	142.29	108.22	4.01

n/d not detectible

n/e not enough sample for analysis

Blending of two homopolymers were done to ascertain the possible effects the polymers will have on each other during crystallisation either in a heterogeneous environment onto sand or a homogeneous environment in solution. Direct comparison of the weight of polymer eluting at each fraction is not possible unless the weighted fraction is taken. When a blend is made of two individual polymers, and no co-crystallisation effects are present, the weighted fraction of the blend should be the average of the two original polymers and can thus be calculated. The weighted fractions of the homopolymers, M-iPP 1 and M-iPP4, and blend as well as the calculated value for the blend are plotted against elution temperature in Figure 5.6.

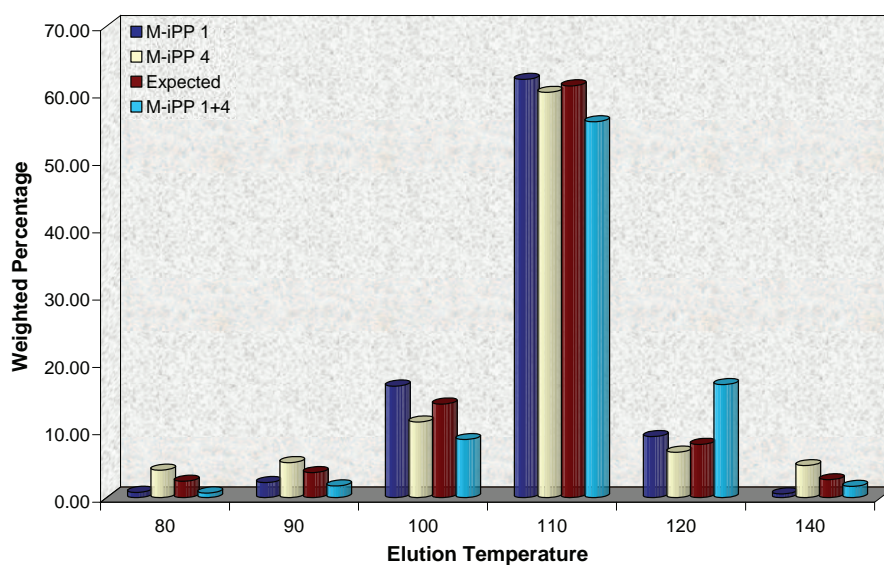


**Figure 5.6:** Weighted Fraction versus elution temperature for M-iPP 1+4

The fact that the calculated and experimentally obtained values do not correspond is an indication that the individual polymers have an influence on each other during crystallisation. Blending of two homopolymers with differing molecular weights effectively increases the PDI. The main fractions for the M-iPP 1+4 blend elutes between 100 °C and 120 °C. The 120 °C experimentally obtained fraction is the only one of these three fractions that has more polymer eluting than the calculated value. This must mean that during the crystallisation step of TREF the combination of the two individual polymers causes a change in the mechanism of crystallisation. Fractions that will crystallise at a lower temperature in the individual polymers now crystallises at a higher temperature in the blend. It is not only the weighted fractions of the blends that are expected to be an average value but also the molecular weight.

As is expected the  $\overline{M}_w$  for the blend fractions falls between the values of the two original polymers but not always the exact average. In the 120 °C fraction, Figure 5.7 it can be seen that the  $\overline{M}_w$  for the blend is higher than average but in the 100 °C and 110 °C fractions it is lower. This suggests that some polymer that crystallised at a lower temperature in the homopolymers is now crystallising at a higher temperature in the blend which is reflected in the weighted fractions eluting. It seems thus that during crystallisation of the blend the higher molecular weight chains crystallise out faster than in the homopolymers. This could be that some polymer starts to crystallise and then act as a nucleus for crystallisation for other polymer chains with the same chemical nature.

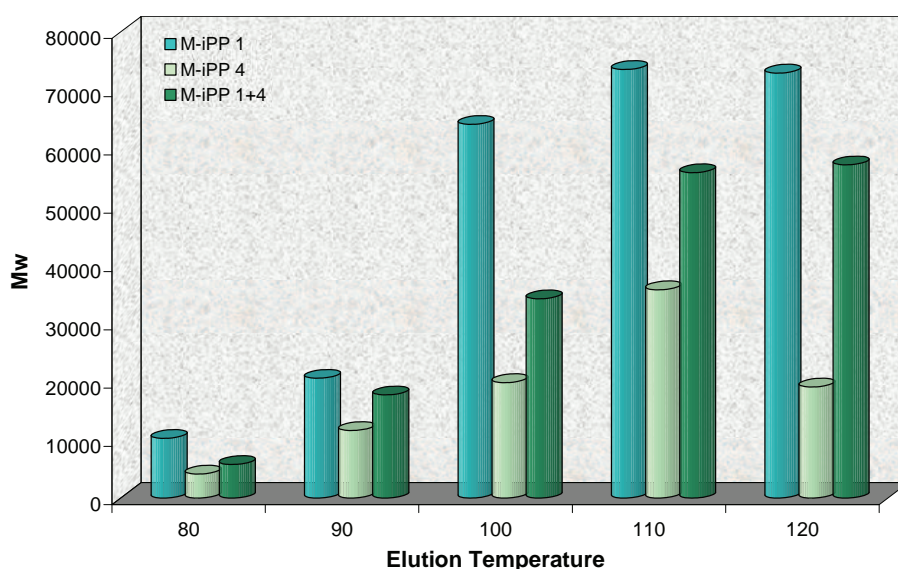


**Figure 5.7:**  $\overline{M}_w$  versus elution temperature for the M-iPP 1+4 blend and homopolymers

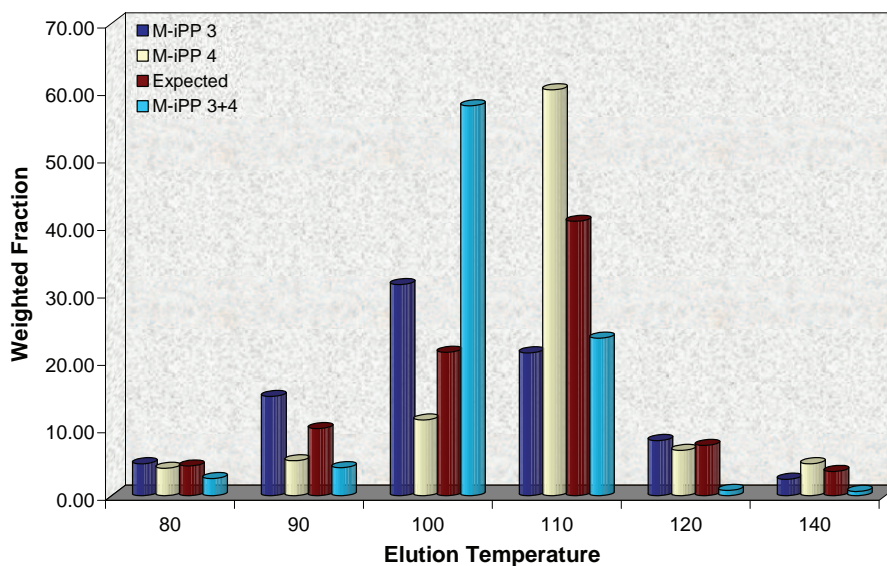


**Figure 5.8:** Weighted Fraction versus elution temperature for M-iPP 3 + 4

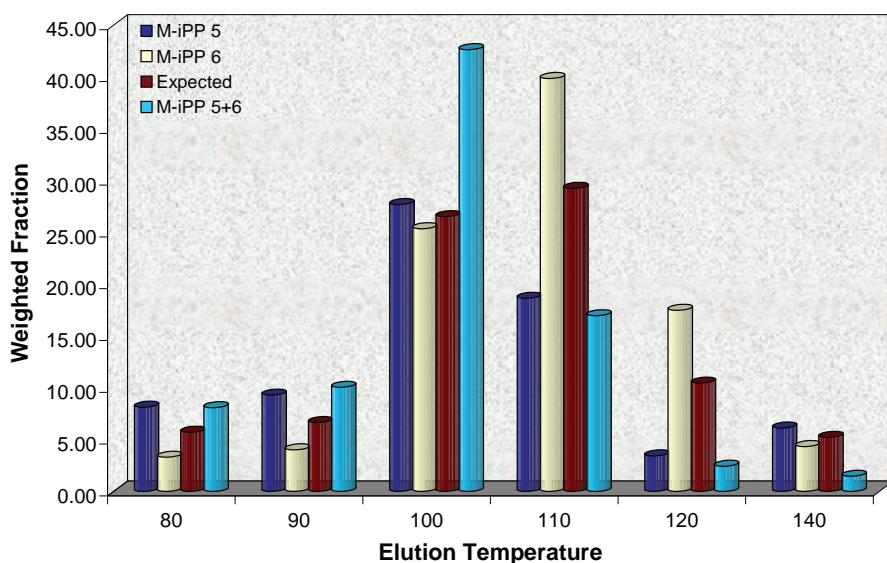


**Figure 5.9:** Weighted Fraction versus elution temperature for M-iPP 5 + 6

In the case of the blend of polymers 3 and 4, a more remarkable shift is seen, as much more polymer is eluting at 100 °C than expected, while much less is eluting at 110 °C. This indicates a mechanism which causes more polymer to crystallise at a lower temperature. The bulk polymers are similar in molecular weight, but dissimilar in PDI and tacticity. While the reason is not clear, the influence of blending on the crystallisation is once again evident. Exactly the same trend is seen for a blend of samples 5 and 6.

Crystallisation can either occur homogeneously, in solution, or heterogeneously, onto sand. To investigate the solution crystallisation, we used the TFA which was developed (see Chapter 4).

## 5.2 Turbidity Data

A typical response for a cooling experiment performed on the turbidity fractionation analyser (TFA) is shown in Figure 5.10. The decrease in the signal is due to increasing scatter from the incident beam due to formation of crystallites during cooling.

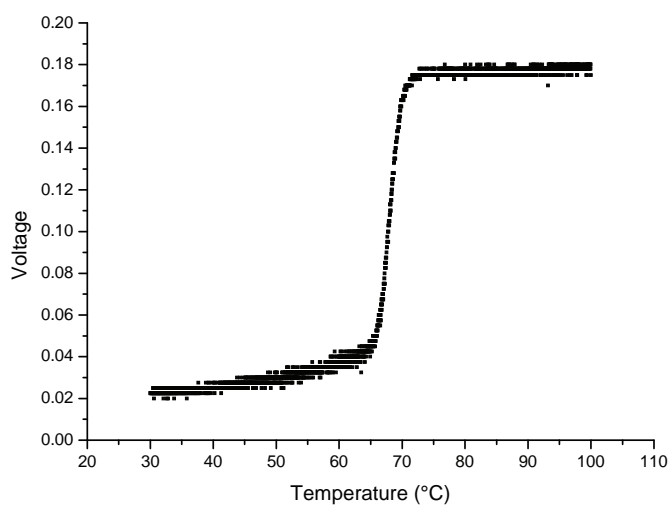


**Figure 5.10:** Typical Response of a cooling experiment with the turbidity analyser

The first derivative is needed to obtain peak width and peak maxima that can be analysed and compared between different samples. Origin<sup>®</sup> software was used for further analysis. Figure 5.11 shows the typical shape graph that is obtained for the first derivative. Extensive scattering before and after crystallisation doesn't have any relevance to this study and to simplify overlay graphs for easier interpretation additional smoothing was performed on these areas.

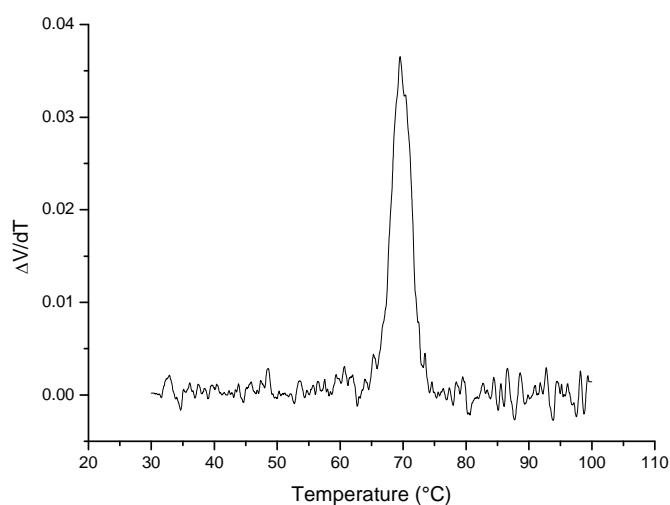


**Figure 5.11:** First derivative of the turbidity data

Blends were made, as mentioned above, from the homopolymers consisting of the same isotacticity but differing in molecular weight. The same blends were used for turbidity experiments to investigate possible molecular weight effects during solution crystallisation. Turbidity fractionation analyses were also done on the homopolymers. The overlay in Figure 5.12 is for the two original homopolymers M-iPP-5 and M-iPP-6 and the blend of the two homopolymers.

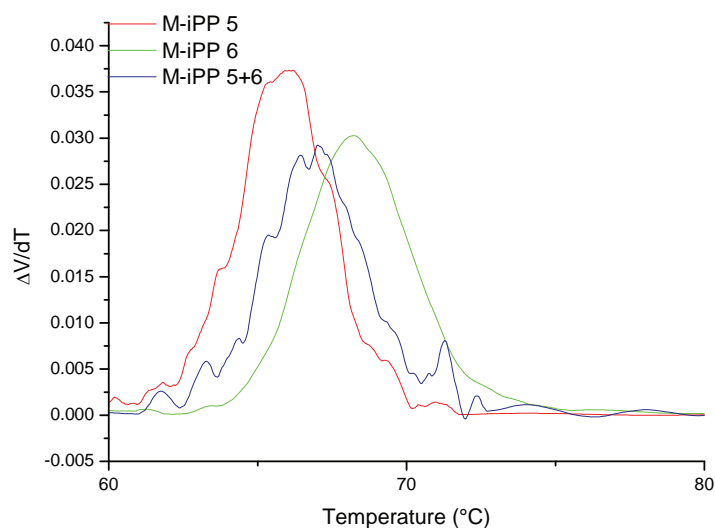


**Figure 5.12:** Overlay of the original homopolymers, similar tacticity different Mw, and the corresponding blend from the TFA data



When we compare the crystallisation from solution for M-iPP-5 and M-iPP-6 (different molecular weight, same tacticity, Table 5.1) we see that the crystallisation temperature (peak temperature) for M-iPP-6, the highest molecular weight polymer, is higher than for M-iPP-5. This appears to be a molecular weight effect. PP crystallises heterogeneously and the high molecular weight appears to crystallise onto nuclei more easily than the lower molecular weight material. The blend of the two materials crystallise over a much broader region than the two individual polymers, and the complexity of the crystallisation profiles seem to reflect the peaks of the individual polymers. Nevertheless, there is a shift to a lower crystallisation temperature for the blend, which indicates the fact that we have a more complex mixture of molecular species present in the blend which influences the crystallisation behaviour of the polymers from solution.

In the case of the M-iPP-3 and M-iPP-4 polymers, we see that with similar molecular weights, the polymer with the highest tacticity crystallises first from solution. Once again, the blend crystallises at a lower temperature than that of M-iPP-4. The difference in crystallisation temperatures must be an indication that the turbidity analyser can distinguish between polymers with different isotacticities.

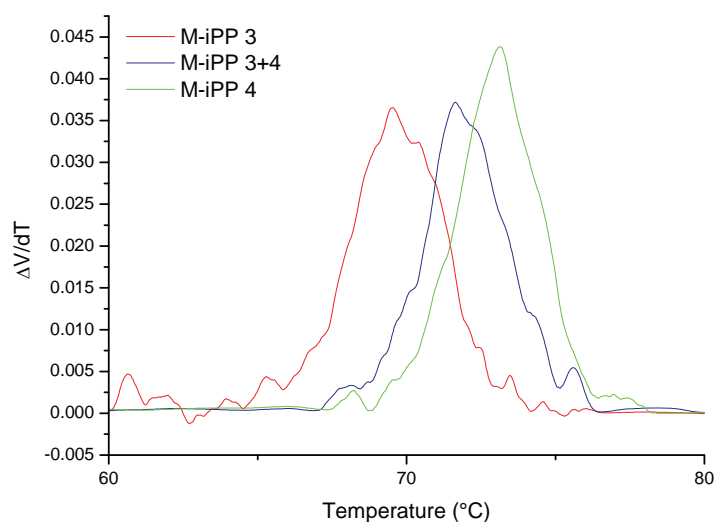


**Figure 5.13:** Overlay of the same Mw differing tacticity

When Comparing M-iPP1 and M-iPP-4 where both the molecular weight and tacticity are different, M-iPP-4 (lowest Mw but highest tacticity) crystallises out of solution at the highest temperature indicating that tacticity effects possibly dominates the crystallisation in this case.

The blend yet again crystallises at a lower temperature than M-iPP-4 indicating again that the blending of the polymers has an influence on the crystallisation.

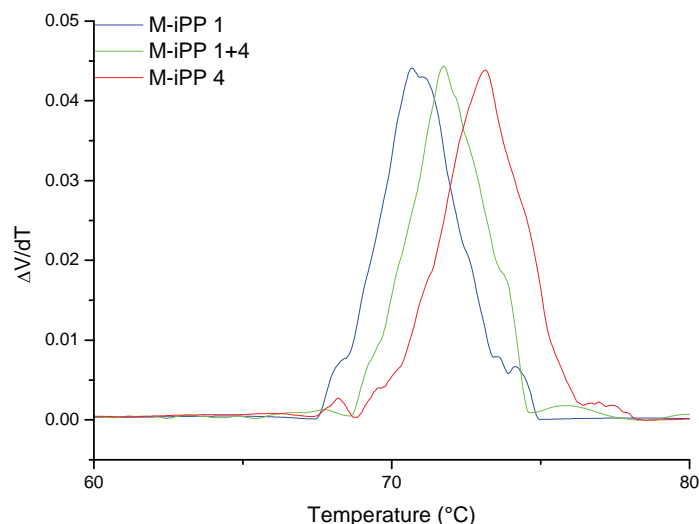


**Figure 5.14:** TFA of two samples with differing Mw and tacticity

It is clear from the TREF results that the metallocene catalysed polymers have a broader than expected molecular species distribution. While both the TREF and turbidity analyser experiments clearly indicate that blends of the polymers do affect the crystallisation behaviour, it is difficult to state exactly what is causing this, as polydispersity and tacticity distribution effects also play a role. In order to see what could be achieved by the TFA, the TREF fractions obtained at 100 °C and 110 °C, from both the individual polymers as well as the blends, were analysed by TFA. Subsequently blends of the fractions obtained from selected individual polymers were blended and analysed by TFA.

First, the individual fractions obtained from TREF (100 °C and 110 °C fractions) for the M-iPP-1, M-iPP-4 and M-iPP-1 + 4 blend were investigated. The TFA overlays are plotted in Figure 5.15 and Figure 5.16 respectively.

The 100 °C fractions of M-iPP-1 have a higher molecular weight (64 109 g/mol vs 19 817 g/mol) but a lower tacticity (93% vs 95%) than the 100 °C fraction of M-iPP-4. The latter has a higher solution crystallisation temperature and it seems that the higher tacticity dominates the solution crystallisation in this case.

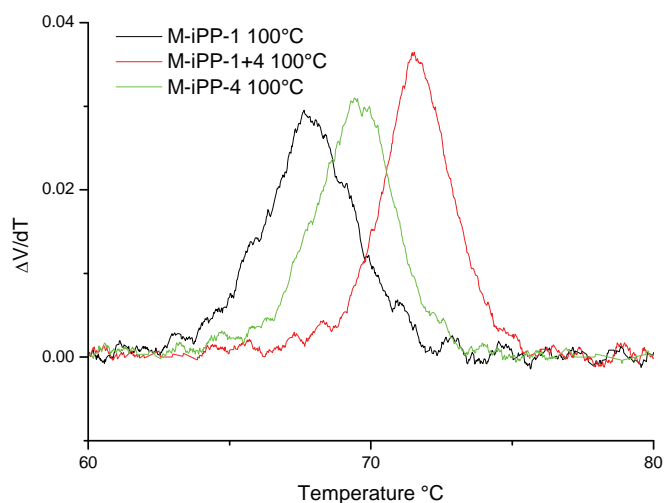


**Figure 5.15:** TFA experiment on the 100°C fractions for M-iPP-1, M-iPP-4 and M-iPP-1+4

In the case of the 110 °C fraction of M-iPP-1 it has both a higher molecular weight (75 517 g/mol vs 35 734 g/mol) as well as higher tacticity (93% vs 89%) than the 110°C of M-iPP-4. This is reflected in the higher solution crystallisation temperature of the former. The solution crystallisation temperature of the fraction eluted at 110 °C of the blend of the materials is a little higher than that of M-iPP-1.

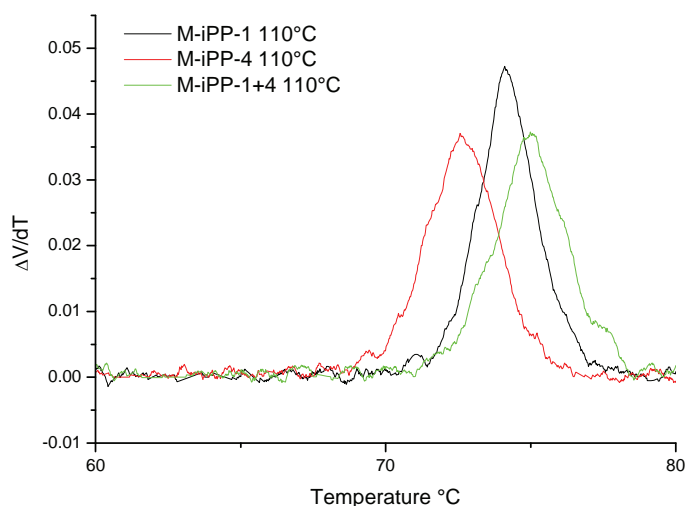


**Figure 5.16:** TFA experiment on the 110°C fractions of the homopolymers and blend

The 100 °C fractions for M-iPP-3 (25 370 g/mol) and M-iPP-4 (19 817 g/mol) have about the same solution crystallisation temperature but the 100 °C fraction of M-iPP-3+4 (56 316 g/mol) has a substantial higher solution crystallisation temperature. The tacticity of M-iPP-4 and M-iPP-3+4 is 95%. In this case it seems that the large difference in molecular weight is the dominating effect in the solution crystallisation. In all of these cases it must be remembered that we are comparing samples that were obtained from TREF for the individual polymers as well as the blends.

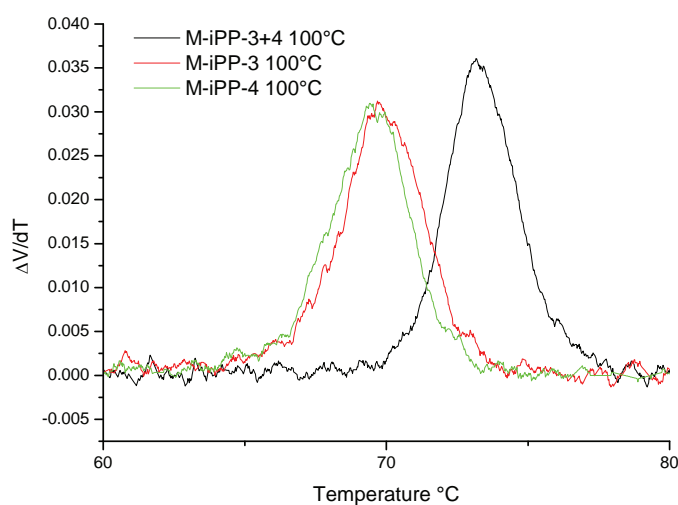


**Figure 5.17:** TFA cooling experiment on the 100 °C fractions of M-iPP-3, M-iPP-4 and M-iPP-3+4

M-iPP-3 (24 262 g/mol), M-iPP-4 (35 734 g/mol) and M-iPP-3+4 (58 503 g/mol) show three distinctly different solution crystallisation temperatures. The tacticity of M-iPP-3+4 is 99% and is most likely the dominant factor in the solution crystallisation leading to a high crystallisation temperature in this case.

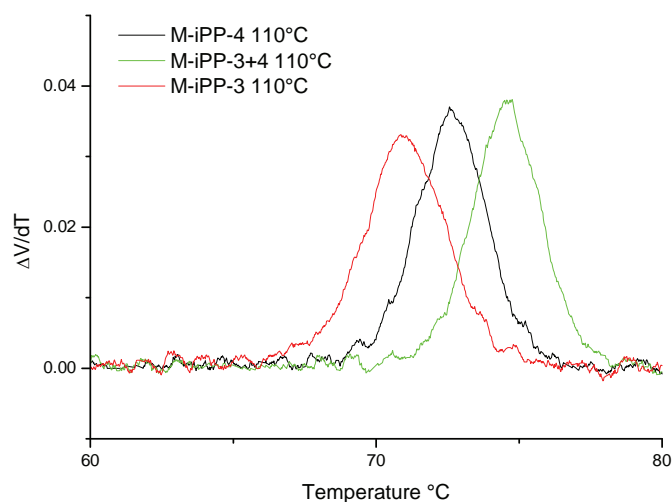


**Figure 5.18:** TFA cooling experiment on the 110°C fraction of M-iPP-3, M-iPP-4 and M-iPP3+4

Up to now the TREF fractions, including the blends were run on the TFA with fractions that were obtained directly from the TREF experiments. To ascertain the effect the fractions will have on each other, blends were made of the fractions (obtained from TREF) of the homopolymers. First a blend was made of the 110 °C fractions obtained from M-iPP-3 and M-iPP-4, illustrated in Figure 5.19. The solution crystallisation temperature of the blend is also higher than the two original materials. A broader crystallisation peak is observed for the blended fractions in comparison with the corresponding blend fraction obtained from TREF. This is an indication of a broader variety of molecular species present in the blend in comparison with the blend fraction obtained from TREF.

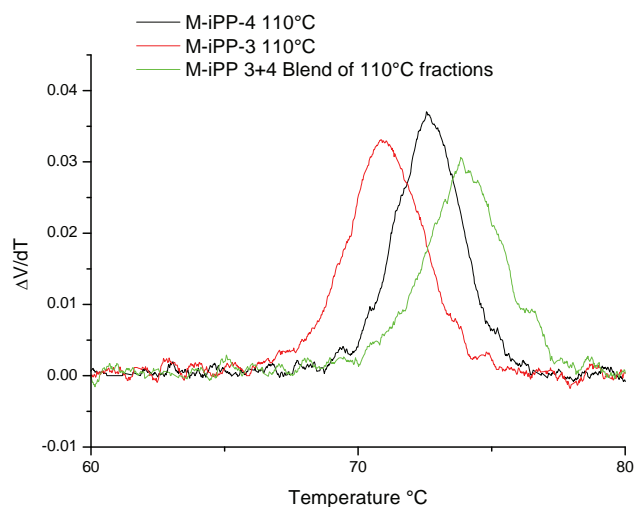


**Figure 5.19:** TFA experiment on the 110 °C fraction of the M-iPP-3 and M-iPP-4 polymer as well as the subsequent blend

In Figure 5.20 the overlay for the 100 °C fraction of M-iPP-5 (35 063 g/mol), M-iPP-6 (82 098 g/mol) and M-iPP-5+6 (80 896 g/mol) is shown. In this case the solution crystallisation temperature for the blend falls between the two original materials. The tacticity for the three fractions is 88%, 91% and 84% respectively. M-iPP-6 with the highest molecular weight and tacticity also crystallises at the highest temperature, which is expected. The tacticity of the M-iPP-5+6 fraction is lower than the corresponding M-iPP-5 fraction but the molecular weight is more than double that and thus seem to dominate the crystallisation.

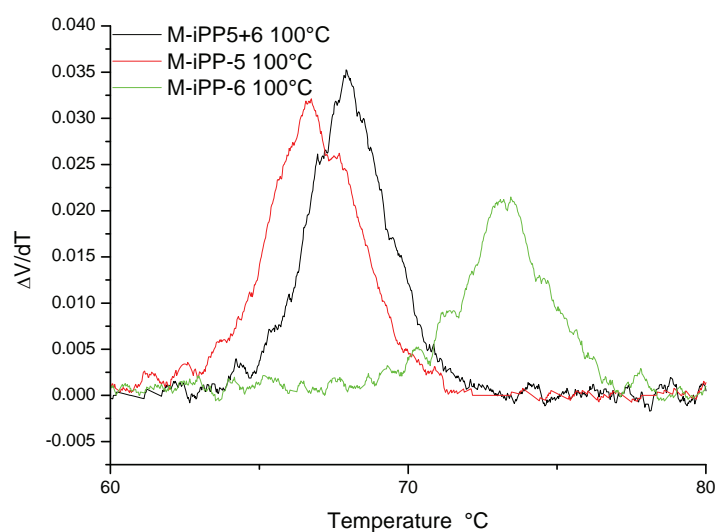


**Figure 5.20:** TFA experiments of the 100°C fraction of M-iPP-5, M-iPP-6 and M-iPP5+6

The molecular weight of the M-iPP-5 and M-iPP-6 110°C fractions are 28117 g/mol and 114570 g/mol respectively while the corresponding isotacticity is 92% and 89%. The molecular weight of the M-iPP-5+6 fraction is 53 248 g/mol with an isotacticity of 89%. M-iPP-6 crystallises out of solution at the highest temperature which is probably due to the comparatively high molecular weight. M-iPP5+6 crystallises out of solution at a higher temperature relative to the 110°C fraction of M-iPP-5 even though the tacticity is lower. The higher crystallisation temperature can be attributed to the higher molecular weight of the fraction.

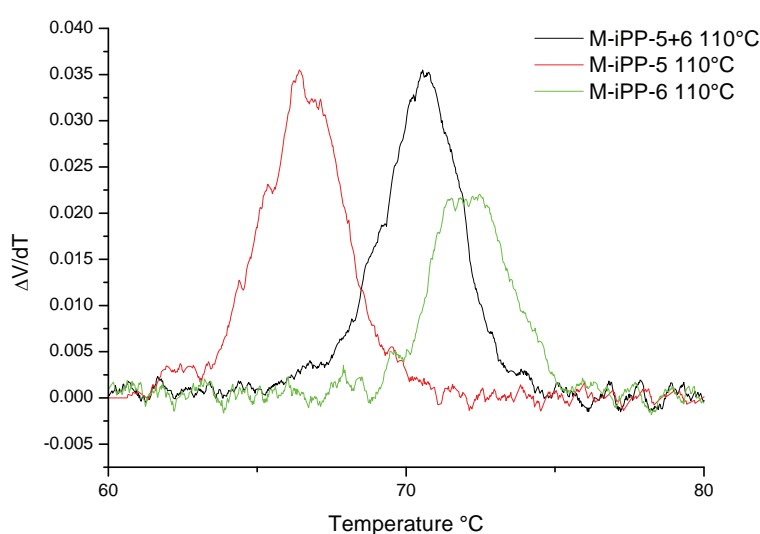


**Figure 5.21:** TFA experiment of the 110°C fraction of the M-iPP-5, M-iPP-6 and M-iPP-5+6 polymers

A blend was made of the 110 °C fraction of M-iPP-5 and M-iPP-6, shown in Figure 5.22. The blend of the two fractions crystallised out of solution a bit lower than the M-iPP-6 fraction but at a higher temperature than the corresponding blend fraction obtained from TREF shown in Figure 5.21. The higher crystallisation temperature could be due to the M-iPP-6 fraction having a greater influence on the blend. The multiplicity of the peak is an interesting phenomenon. The peak shape of the blend definitely mimics the original fractions.

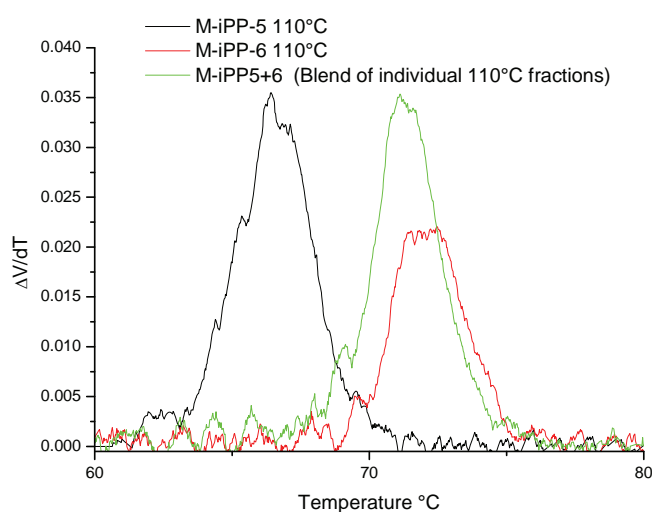


**Figure 5.22:** TFA experiment of the 110°C fraction of the homopolymers and a blend of it

### 5.3 Summary

The studies on the blends of materials with well-defined molecular weights and tacticities indicate that molecular weight, as well as molecular weight distribution does play a role in the crystallisation of isotactic polypropylene. The TFA gives further insight into this phenomenon, and while stereoregularity plays a big role in the crystallisation of these polymers, it is clear that the role to the molecular weight cannot be ignored. This is also evidenced by the fact that blending of two polymers with similar tacticities and different molecular weight results in crystallisation behaviour that is different from the individual polymers. This was also shown by the TFA experiments when individual TREF fractions were blended in solution and cooled.



## 5.4 References

- (1) Busico, V.; Cipullo, R.; Monaco, G.; Vacatello, M. *Macromolecules* **1997**, *30*, 6251-6263.
- (2) Wild, L.; Ryle, T. R.; Knobloch, D. C.; Peat, I. R. *J. Polym. Sci., Polym. Phys. Ed.* **1982**, *20*, 441-455.
- (3) Arranz-Andrés, J.; Peña, B.; Benavente, R.; Pérez, E.; Cerrada, M. L. *Eur. Polym. J.* **2007**, *43*, 2357-2370.
- (4) Lu, H.; Qiao, J.; Xu, Y.; Yang, Y. *J. Appl. Polym. Sci.* **2002**, *85*, 333-341.
- (5) Lehtinen, A.; Paukkeri, R. *Macromol. Chem. Phys.* **1994**, *195*, 1539-1556.

# Chapter 6

## Conclusions and recommendations

*In this chapter all conclusions are summarised and recommendations for further work are suggested.*

## 6.1 Conclusions

6.1.1. A series of isotactic polypropylenes were successfully synthesized. These polymers differed significantly in molecular weight.

6.1.2. The isotactic polypropylene materials were fully characterised and then fractionated by preparative TREF. Characterisation revealed that the polymers were not as homogenous in character as we had expected. Some polymers had a broad molecular weight distribution and showed indications of greater than expected 2, 1 and 1, 3 misinsertions.

6.1.3. Blending of the homopolymers and subsequent fractionation by TREF of the blends were done. The TREF fractions were characterised, and compared to the TREF fractions of the individual polymers at the same elution temperature. It was clear that crystallisation in the blends was different than in the individual polymers. Both the nature and amounts of material isolated at comparable elution temperatures were different to what could be expected if there was no co-crystallisation effect in the blends.

6.1.4. To further study this effect a turbidity fractionation analyser was developed and tested. In the development stage it was firstly ascertained that the analyser can indeed distinguish between different polymers. Thereafter the same polymers and blends of polymers used in the TREF were analyzed. The blends of the homopolymers also showed a shift in solution crystallisation temperature relative to the homopolymers. As mentioned before the synthesised homopolymers was not as homogeneous as hoped for.

6.1.5. After TREF fractionation the fractions obtained were quite homogeneous and thus these fractions were also run on the TFA to ascertain possible effects influencing solution crystallisation. The fractions obtained from TREF of the blends were also run. Blending of the fractions obtained from the fractionated homopolymers was also done and definite shifts in the solution crystallisation temperature were seen. There was no single parameter determining the shift but it was either the tacticity or the molecular weight of the polymer influencing the shift. In the case where the tacticity was the same the molecular weight was the factor influencing the shift. When there was a difference in tacticity it was usually the highest tacticity polymer crystallising out of solution first. There was, however, an exception where the difference in molecular weight was so large that it dominated the crystallisation. In that case even though the tacticity for the high molecular weight polymer was lower than the other fraction in the blend it crystallised out of solution at a higher temperature. It was ascertained that when a blend of the homopolymers was made, the two homopolymers definitely affect each other and shifts in the solution crystallisation temperature occurred. The cause of these shifts was either a tacticity effect or a molecular weight effect.

Overall, the two main aims of the study was met; a turbidity analyzer was designed and constructed, and the molecular weight effect during crystallisation from solution was investigated, and in the materials that were selected for this study, it is clear that molecular weight plays a role during the crystallisation process.

## **6.2 Recommendations**

Further development of the TFA has already begun. A large amount of information can be gleaned from this instrument, including the kinetics of crystallisation and the rate of crystal growth from solution.

With regards to the effect of molecular weight on crystallisation, this work can be expanded to polymers of higher molecular weight than those tested in this study. This will indicate if there is a practical limit where molecular weight no longer plays a role. To this end, a new series of isotactic polypropylenes could be synthesized, or commercial iPP could be fractionated in more well defined fractions by TREF and those fractions used in TFA experiments. The investigation of syndiotactic polymers can also be undertaken.

## Appendix A

### NMR data

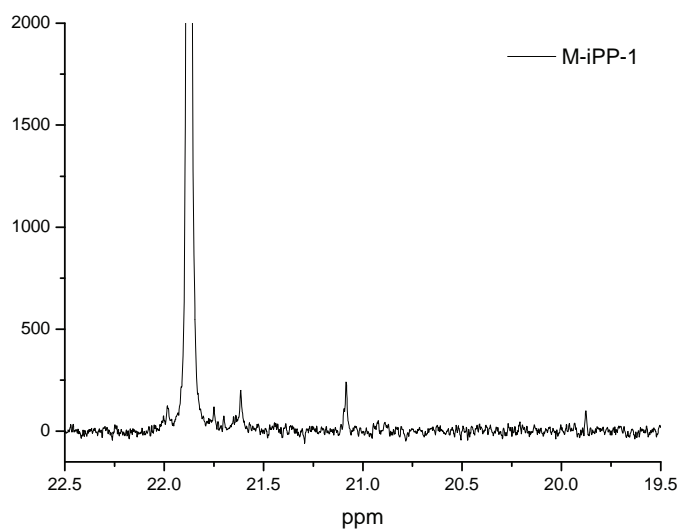


**Figure A.1:** NMR spectrum of the unfractionated M-iPP-1 homopolymer.

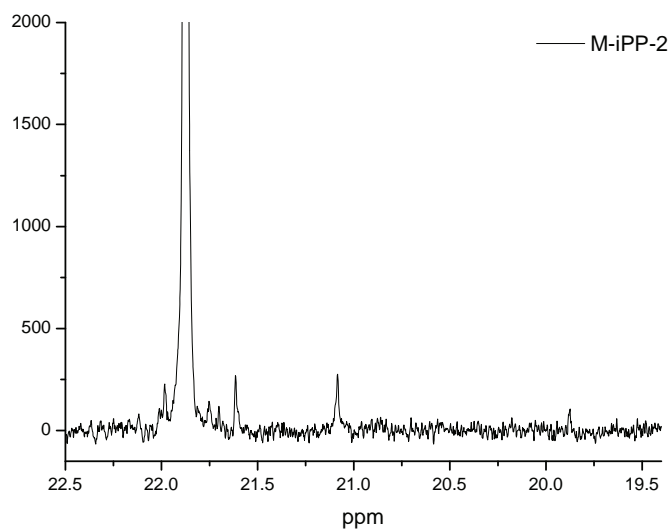


**Figure A.2:** NMR spectrum of the unfractionated M-iPP-2 homopolymer.

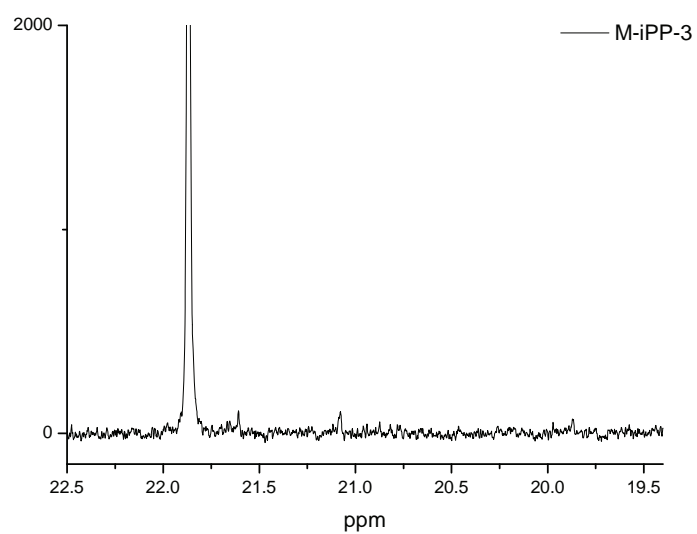


**Figure A.3:** NMR spectrum of the unfractionated M-iPP-3 homopolymer

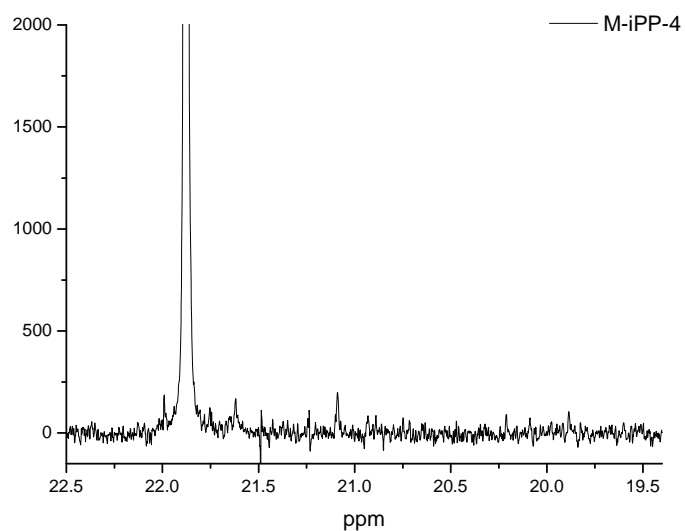


**Figure A.4:** NMR spectrum of the unfractionated M-iPP-4 homopolymer.

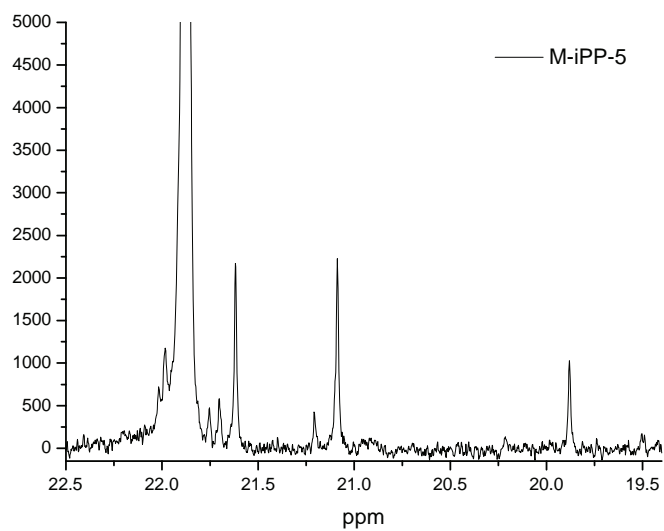


**Figure A.5:** NMR spectrum of the unfractionated M-iPP-5 homopolymer.

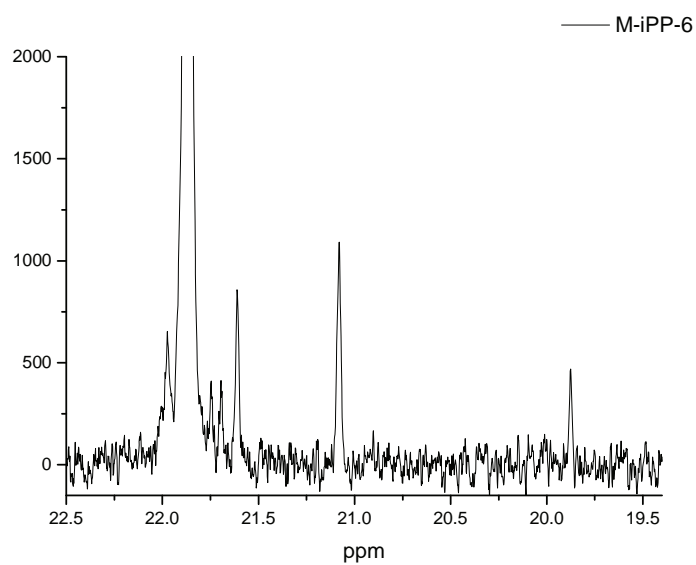


**Figure A.6:** NMR spectrum of the unfractionated M-iPP-6 homopolymer.

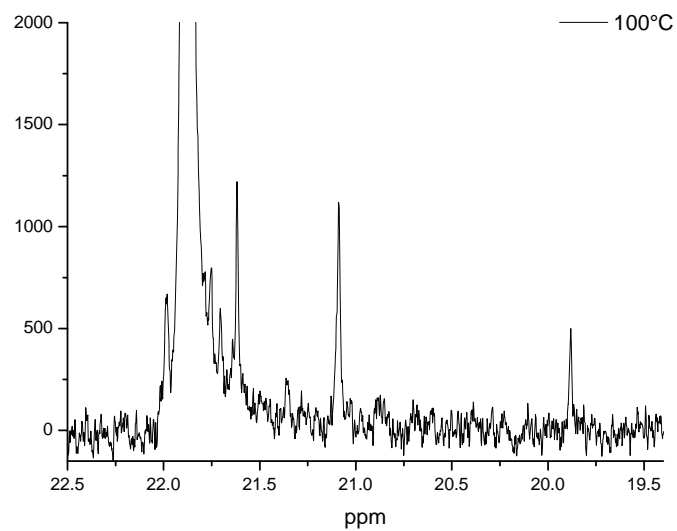


**Figure A.7:** NMR spectrum of the 100°C fraction of the M-iPP-2+3 blend

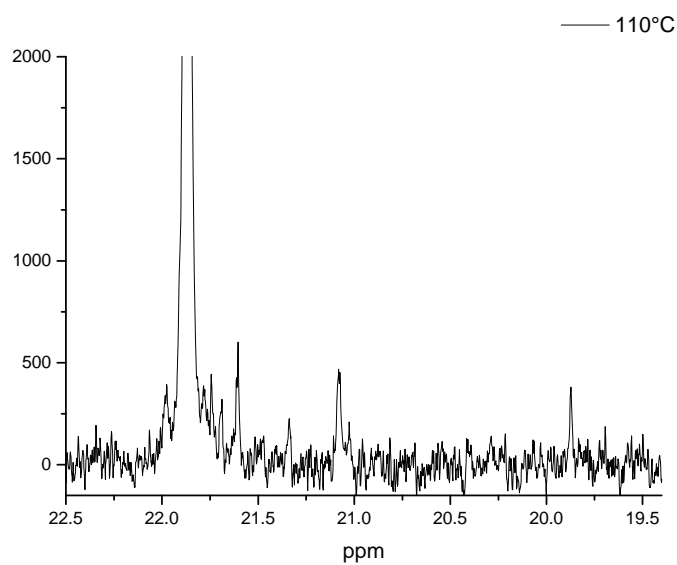


**Figure A.8:** NMR spectrum of the 110°C fraction of the M-iPP-2+3 blend



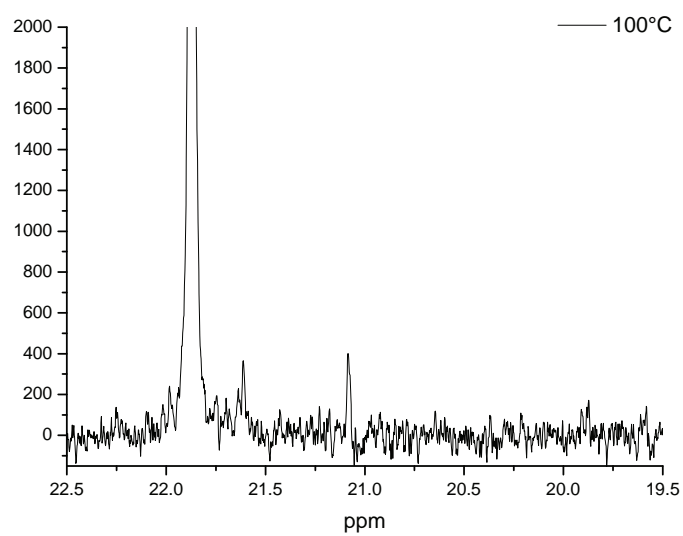


**Figure A.9:** NMR spectrum of the 100°C fraction of the M-iPP-3+4 blend

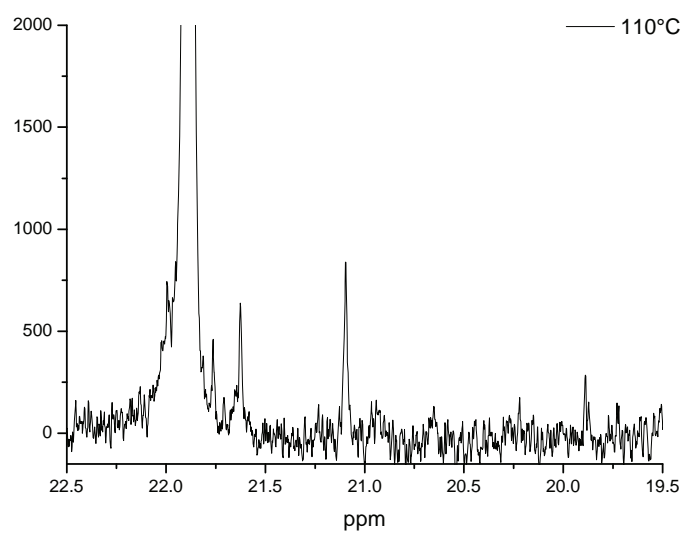


**Figure A.10:** NMR spectrum of the 110°C fraction of the M-iPP-3+4 blend

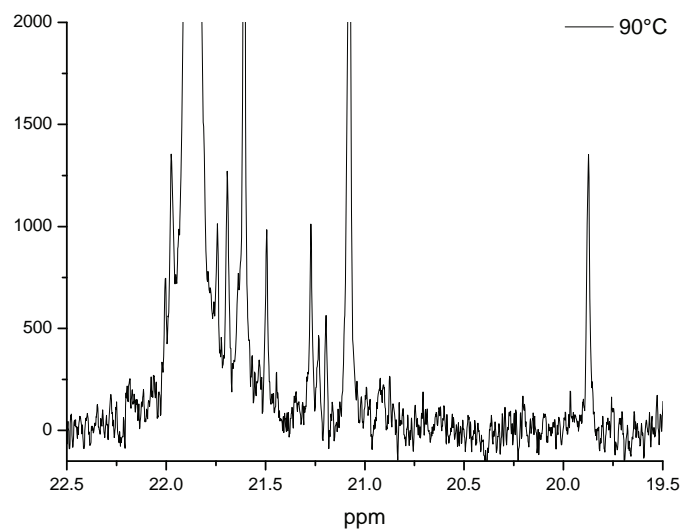


**Figure A.11:** NMR spectrum of the 90°C fraction of the M-iPP-5+6 blend

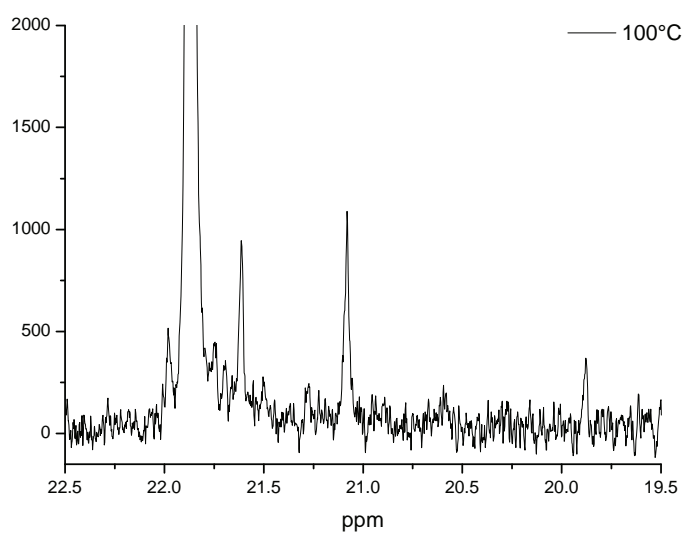


**Figure A.12:** NMR spectrum of the 100°C fraction of the M-iPP-5+6 blend

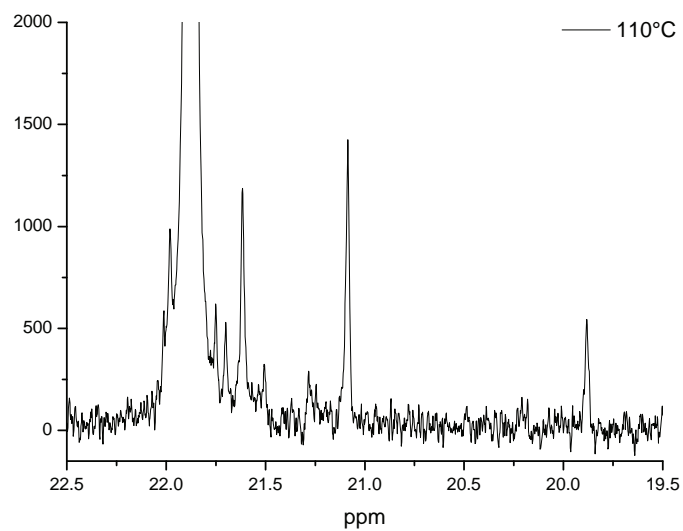


**Figure A.13:** NMR spectrum of the 110°C fraction of the M-iPP-5+6 blend

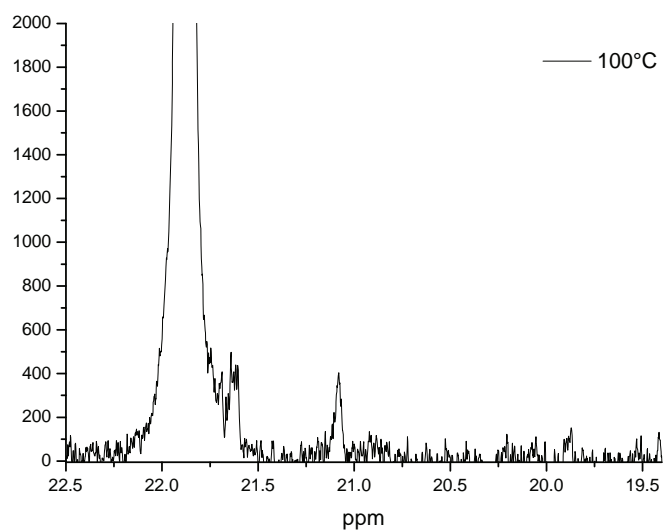


**Figure A.14:** NMR spectrum of the 100°C fraction of M-iPP-1 homopolymer

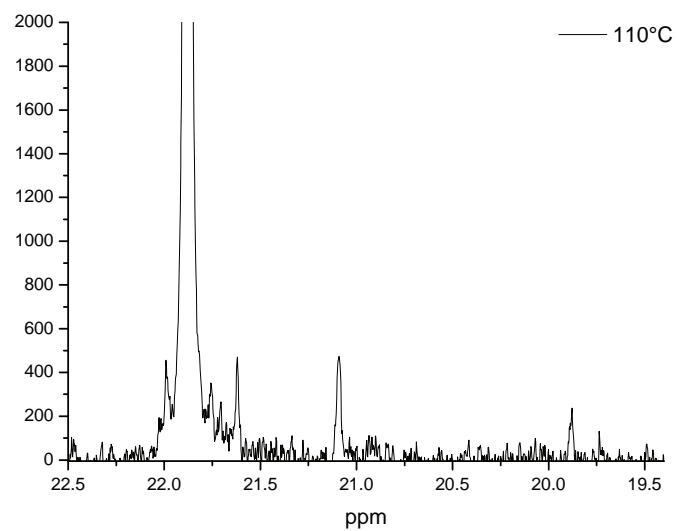


**Figure A.15:** NMR spectrum of the 110°C fraction of M-iPP-1 homopolymer

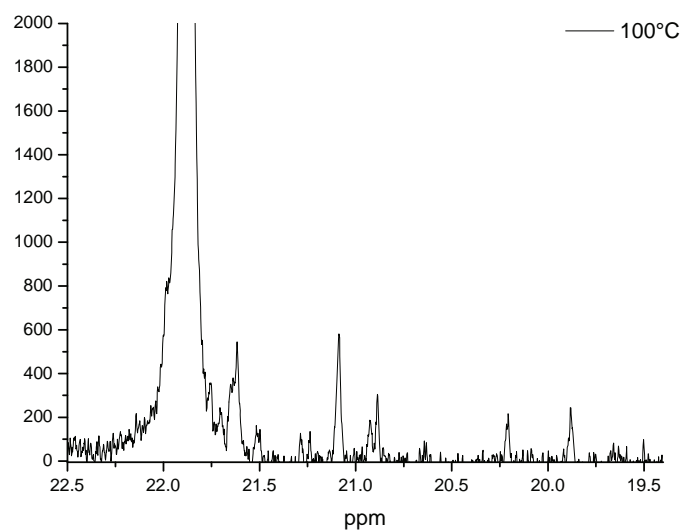


**Figure A.16:** NMR spectrum of the 100°C fraction of M-iPP-4 homopolymer

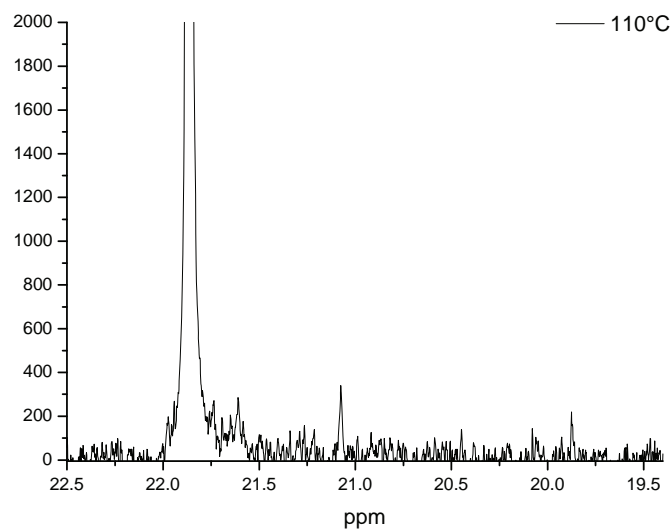


**Figure A.17:** NMR spectrum of the 110°C fraction of M-iPP-4

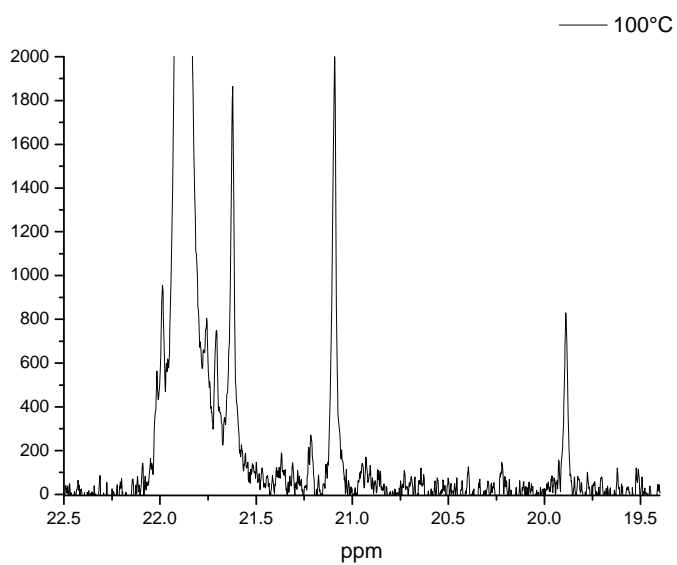


**Figure A.18:** NMR spectrum of the 100°C fraction of M-iPP-5

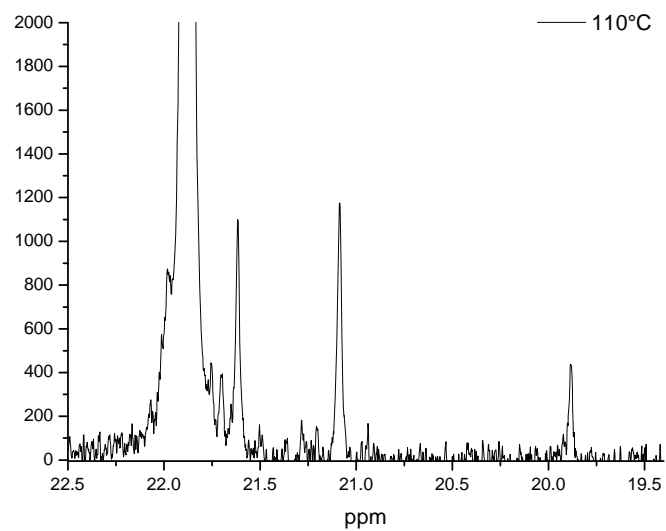


**Figure A19:** NMR spectrum of the 110°C fraction of M-iPP-5

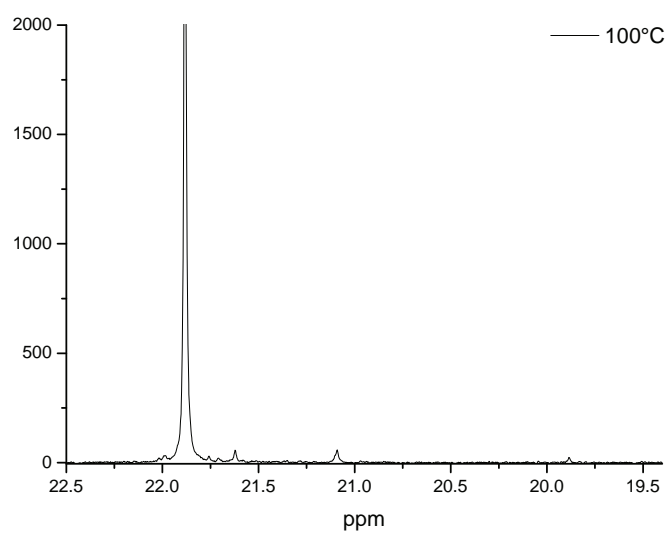


**Figure A.20:** NMR spectrum of the 100°C fraction of M-iPP-6

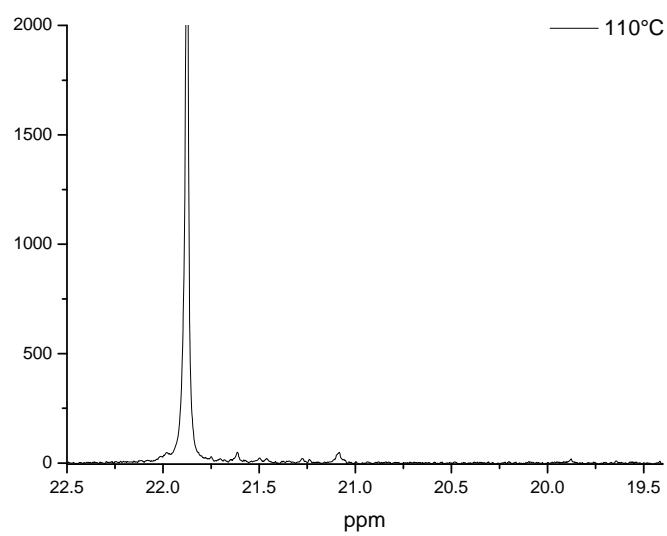


**Figure A.21:** NMR spectrum of the 110°C fraction of M-iPP-6

## Appendix B

### DSC data

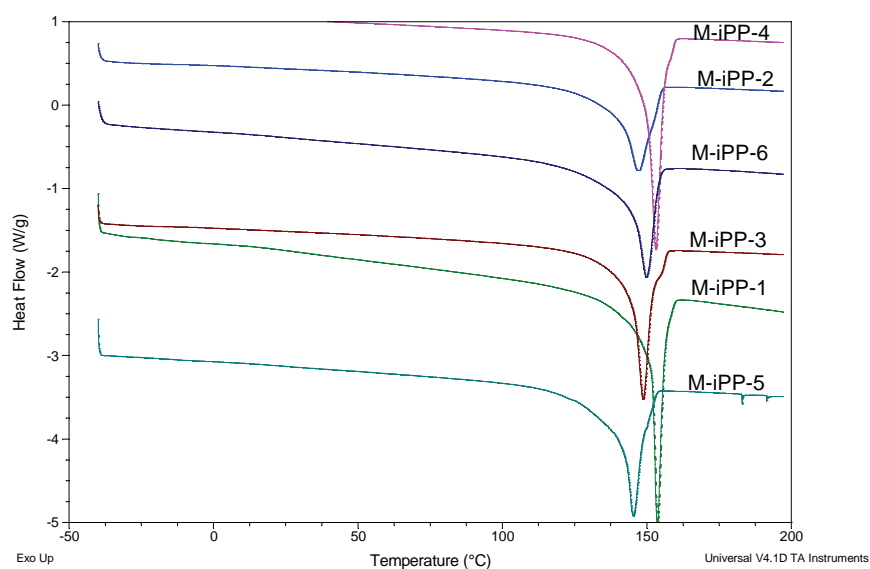


**Figure B.1:** DSC thermogram overlay of the homopolymers

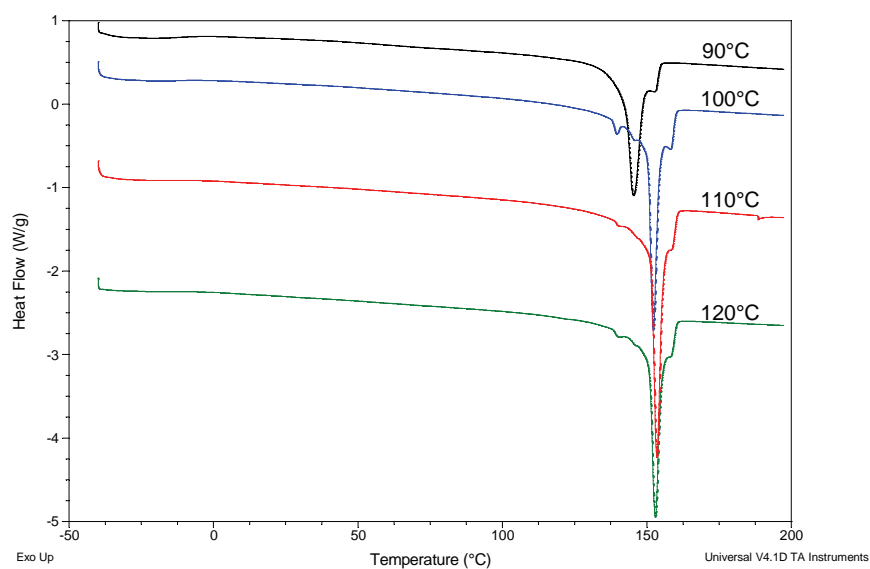


**Figure B.2:** DSC thermogram overlay of the fractions obtained from TREF for homopolymer M-iPP-1



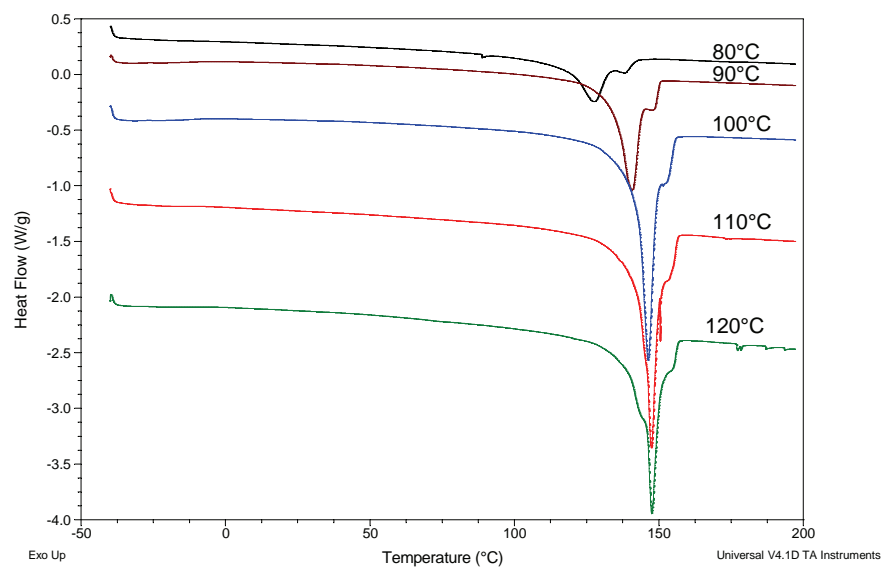


**Figure B.3:** DSC thermogram overlay of the fractions obtained from TREF for the homopolymer of M-iPP-3

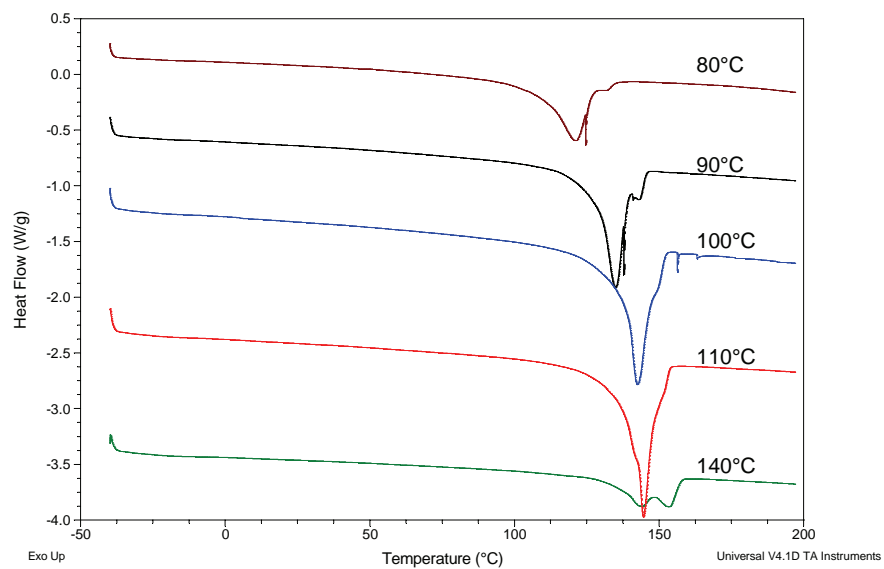


**Figure B.4:** DSC thermogram overlay of the fractions obtained from TREF for the homopolymer of M-iPP-5

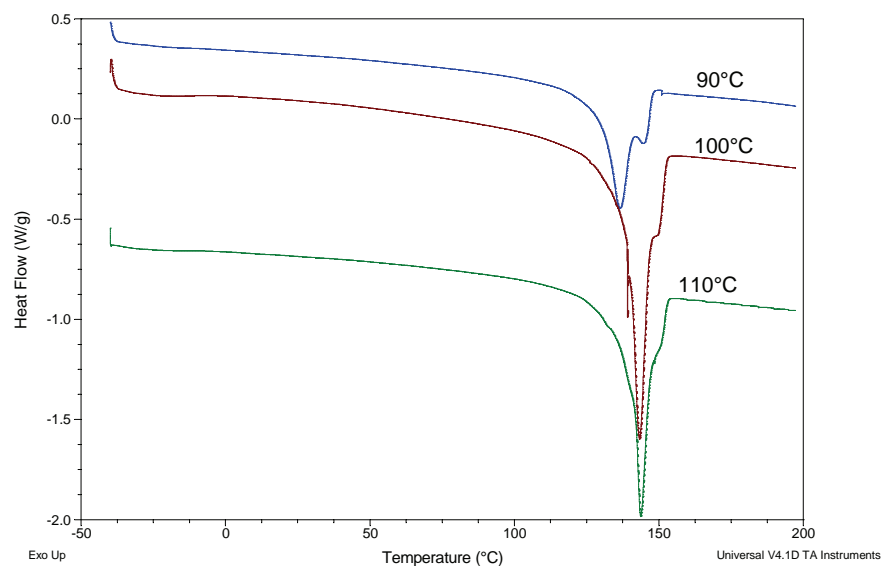


**Figure B.5:** DSC thermogram overlay of the fractions obtained from TREF for the homopolymer M-iPP-6

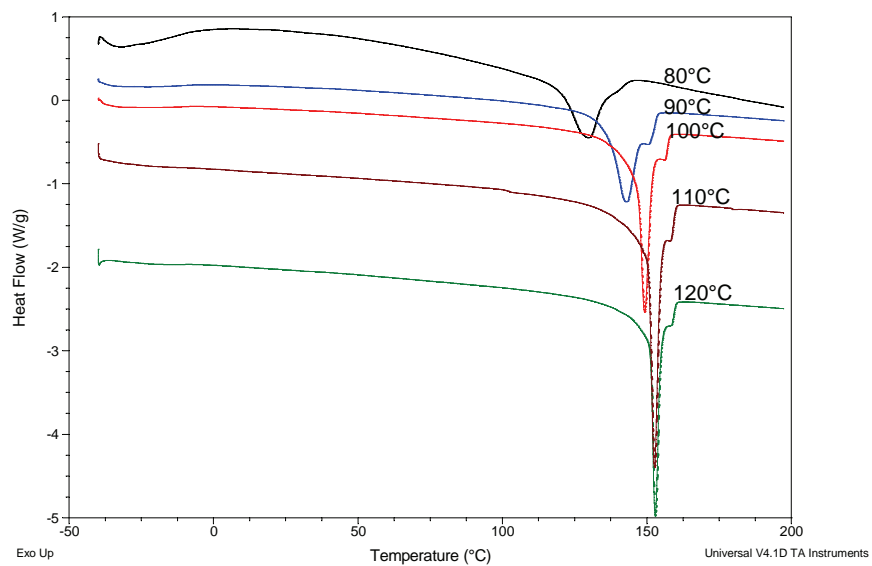


**Figure B.6:** DSC thermogram overlay of the fractions obtained from TREF for the blend of M-iPP-1+4

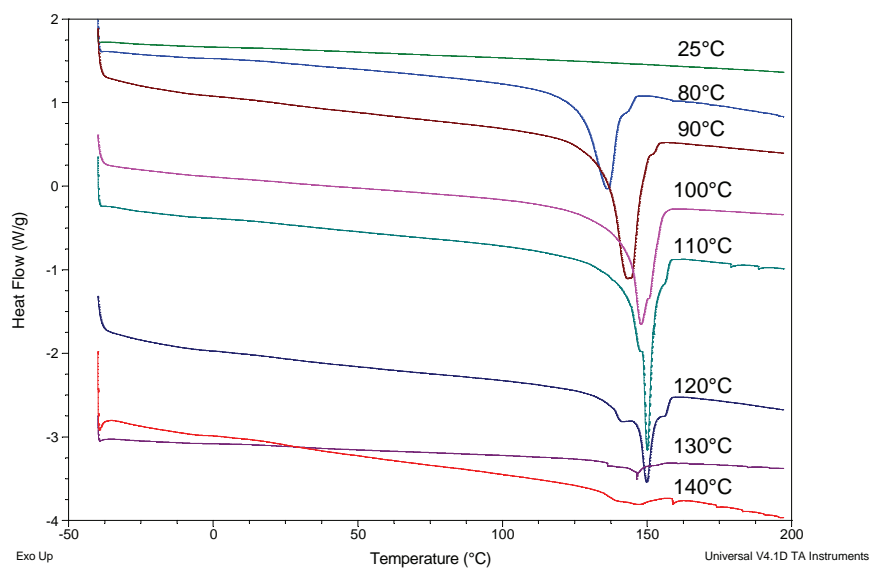


**Figure B.7:** DSC thermogram overlay of the fractions obtained from TREF for the blend of M-iPP2+3

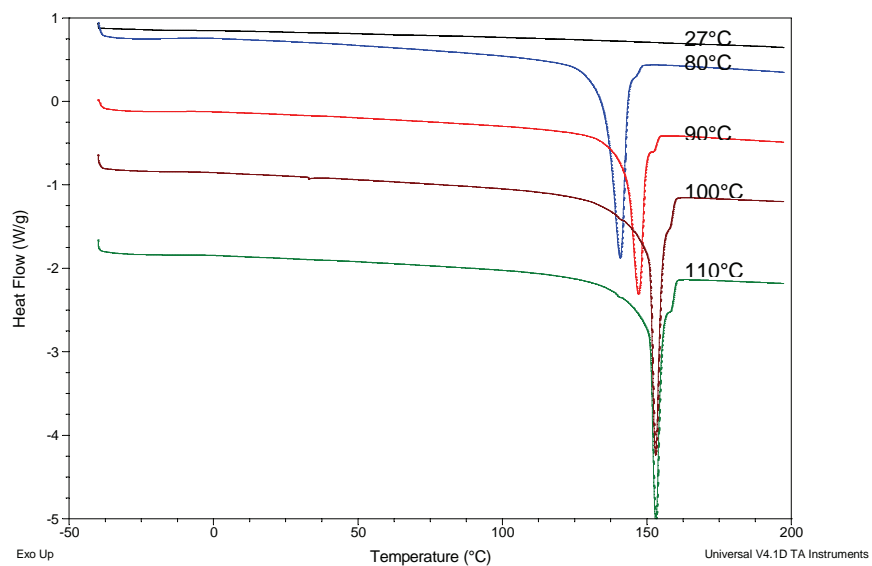


**Figure B.8:** DSC thermogram overlay of the fractions obtained from TREF for the blend of M-iPP-3+4

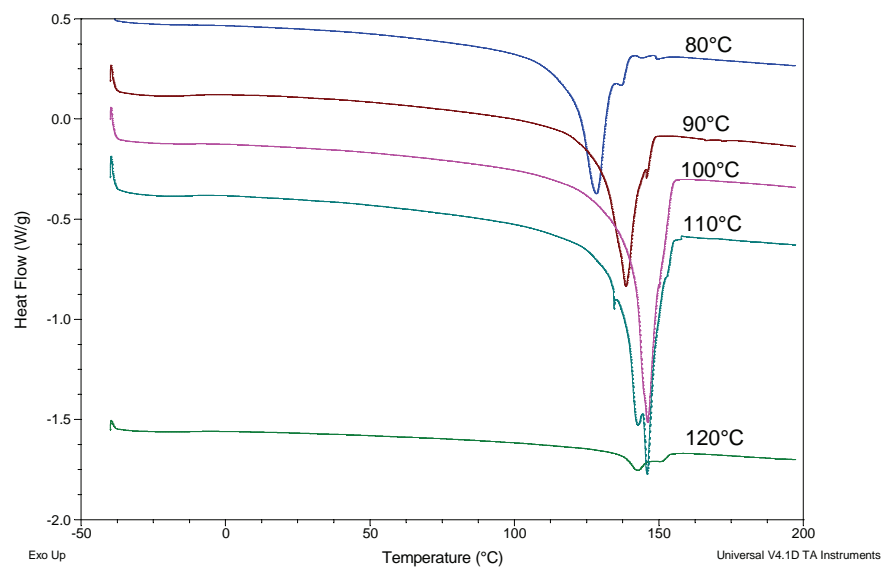


**Figure B.9:** DSC thermogram overlay of the fractions obtained from TREF for the blend of M-iPP-5+6